Higgs coupling constants as a probe of new physics

Shinya Kanemura,[1,*] Yasuhiro Okada,[2,3,†] Eibun Senaha,[2,3,‡] and C.-P. Yuan[4,§]

[1]*Department of Physics, Osaka University, Toyonaka, Osaka 560-0043, Japan*

[2]*Theory Group, KEK, Tsukuba, Ibaraki 305-0801, Japan*

[3]*Department of Particle and Nuclear Physics, the Graduate University for Advanced Studies, Tsukuba, Ibaraki 305-0801, Japan*

[4]*Department of Physics and Astronomy, Michigan State University, East Lansing, Michigan 48824-1116, USA*

(Received 31 August 2004; published 7 December 2004)

We study new physics effects on the couplings of weak gauge bosons with the lightest *CP*-even Higgs boson (h), hZZ, and the trilinear coupling of the lightest Higgs boson, hhh, at the one-loop order, as predicted by the two Higgs doublet model. Those renormalized coupling constants can deviate from the standard model (SM) predictions due to two distinct origins: the tree level mixing effect of Higgs bosons and the quantum effect of additional particles in loop diagrams. The latter can be enhanced in the renormalized hhh coupling constant when the additional particles show the nondecoupling property. Therefore, even in the case where the hZZ coupling is close to the SM value, deviation in the hhh coupling from the SM value can become as large as plus 100%, while that in the hZZ coupling is at most minus 1% level. Such large quantum effect on the Higgs trilinear coupling is distinguishable from the tree level mixing effect, and is expected to be detectable at a future linear collider.

DOI: 10.1103/PhysRevD.70.115002 PACS numbers: 14.80.Cp, 12.15.Lk

I. INTRODUCTION

In the standard picture of elementary particle physics, the electroweak gauge symmetry is spontaneously broken by introducing an isodoublet scalar field, the Higgs field. Its neutral component receives the vacuum expectation value. Consequently, the gauge bosons and the matter fields obtain their masses through the couplings with the Higgs scalar field.

Identification of the Higgs boson is one of the most important goals of high energy collider experiments. The fit by LEP Electroweak Working Group favors a relatively light Higgs boson with its mass below 251 GeV, assuming the standard model (SM) [1]. The search for the Higgs bosons is being carried out at Fermilab Tevatron and will be continued at CERN Large Hadron Collider (LHC). There the SM Higgs boson is expected to be discovered as long as its mass is less than 1 TeV. In order to verify the mechanism of mass generation, the Higgs boson couplings with gauge bosons as well as fermions have to be determined with sufficient accuracy. Moreover, precise determination of the self-coupling constant of the Higgs boson is essential to determine the structure of the Higgs potential. An electron-positron (e^-e^+) linear collider (LC), such as GLC [2], TESLA [3] or NLC [4] and its photon-photon (γ-γ) collider option, can provide an opportunity for the precise measurement of the Higgs boson couplings. At LCs, the Higgs boson (h) is produced mainly via the Higgsstrahlung process $e^+e^- \to Zh$ for relatively low energies and also via the fusion process $e^+e^- \to W^{+*}W^{-*}\nu\bar{\nu} \to h\nu\bar{\nu}$ for higher energies [5]. In both production mechanisms, the Higgs boson is produced through the coupling with weak gauge bosons. The cross sections are expected to be measured at a percent level or better unless the Higgs boson is relatively heavy. The Higgs boson couplings with heavy quarks (except the top quark) and the tau lepton can be tested by measuring the decay branching ratios of the Higgs boson. Furthermore, the trilinear coupling of the Higgs boson hhh [6–15] and the top-Yukawa coupling $ht\bar{t}$ can be determined by measuring the cross section of double Higgs production processes [16–18] $e^+e^- \to Zhh$ as well as $e^+e^- \to W^{+*}W^{-*}\nu\bar{\nu} \to hh\nu\bar{\nu}$ and the top-associated Higgs production process [19] $e^+e^- \to ht\bar{t}$, respectively. The $\gamma\gamma$ option of the LC can also be useful for the Higgs self-coupling measurement [20].

Studying the Higgs sector is not only useful for the confirmation of the breaking mechanism of the electroweak gauge symmetry, but also provides a sensitive window for new physics beyond the SM. In fact, in many models of new physics an extended Higgs sector appears as the low energy effective theory, which has discriminative phenomenological properties. One popular example is known to be the minimal supersymmetric standard model (MSSM) [21], in which the Higgs sector is a two Higgs doublet model (THDM). Some models of the dynamical breaking of the electroweak symmetry also induce more than one Higgs doublet in their low energy effective theories [22]. There are other motivations to introduce extra Higgs fields, such as electroweak baryogenesis [23], top-bottom mass hierarchy [24], and neutrino mass problem [25].

A common feature of extended Higgs sectors is the existence of additional scalar bosons, such as charged Higgs bosons and *CP*-odd Higgs boson(s). After the discovery of the lightest Higgs boson, direct search of these

*Electronic address: kanemu@het.phys.sci.osaka-u.ac.jp
†Electronic address: yasuhiro.okada@kek.jp
‡Electronic address: senaha@post.kek.jp
§Electronic address: yuan@pa.msu.edu

extra scalar particles would become important to distinguish new physics models from the SM. Even if the extra Higgs bosons are not found, we can still obtain insight by looking for indirect effects of the extra Higgs boson from the precise determination of the lightest Higgs boson properties [26]. For example, the mass, width, production cross sections, and decay branching ratios of the lightest Higgs boson should be thoroughly measured to test whether or not these data are consistent with the SM. The existence of extra Higgs bosons can affect the observables associated with the lightest Higgs boson through both the tree level mixing effect and the quantum loop effect. In this way, we might find clues to new physics before finding the extra Higgs bosons from the direct search experiments.

In this paper, we evaluate the Higgs coupling with the gauge boson hZZ and the Higgs self-coupling hhh at one-loop level in the THDM, in order to study the impact of the extra Higgs bosons on the coupling associated with the lightest Higgs boson (h). In Refs. [13,14], the one-loop contributions of additional Higgs bosons and heavy quarks to the hhh coupling were discussed in the limit where only h is responsible for the electroweak symmetry breaking (in the SM-like limit). The calculation had been done both in the effective potential method and in the diagrammatic method, but details of the calculation were not shown. In the present paper, we will show the details of our calculation, in which the on-shell renormalization scheme [27,28] is adopted. In addition, new particle effects on the form factors of the hZZ coupling are also evaluated. Furthermore, we also extend our discussion in Refs. [13,14] for the case of the SM-like limit to more generic cases.

In the THDM, masses of the heavy Higgs bosons can come from two kinds of contributions: the vacuum expectation value v ($\simeq 246$ GeV) and the gauge invariant mass term. When the heavy Higgs boson mass is predominantly generated by v, contributions in powers of the mass of the loop particles can appear in the one-loop effect couplings of hZZ and hhh. They are quadratic for the hZZ coupling and quartic for the hhh coupling [13,14]. In this case, relatively large quantum correction is expected in the hhh vertex, especially when the particle in the loop is heavy. Although similar nondecoupling loop effects can also appear in the THDM [29] in the processes of $h \to \gamma\gamma$ [30,31], $h \to b\bar{b}$ [31], $e^+e^- \to W^+W^-$ [32] and those with the coupling $W^\pm H^\mp V$ ($V = Z, \gamma$) [33], the quartic power contribution of the mass is a unique feature of the hhh coupling. These observables can receive large quantum corrections due to the nondecoupling effects. On the contrary, when the heavy Higgs bosons obtain their masses mainly from the other source, such powerlike contribution disappears and the one-loop effects vanish in the large mass limit. The Higgs sector of the MSSM belongs to this case.

At the tree level, both the hZZ and hhh coupling constants of the THDM can largely deviate from the SM values due to the Higgs mixing effect. The hZZ coupling is given by the multiplication of the factor $\sin(\beta - \alpha)$ to the SM coupling constant, where $\tan\beta$ is the ratio of the vacuum expectation values and α is the mixing angle between CP-even Higgs bosons. In the limit of $\sin(\beta - \alpha) = 1$, where the hZZ coupling recovers the SM value, the hhh coupling also approaches to the SM prediction for a given mass of the Higgs boson h. We study how this correlation can be changed by the one-loop corrections.

We evaluate the one-loop effects due to additional Higgs bosons as well as the top quark under the constraint from the perturbative unitarity [34–36] and the vacuum stability [37]. The constraint from the available precision data such as the ρ parameter constraint is also taken into account [38,39].

The one-loop effect on the hZZ coupling can be as large as minus 1% of the SM coupling in the wide range of parameter space. This shows that a larger negative deviation can only be realized due to the Higgs mixing effect, i.e., the effect of the factor $\sin(\beta - \alpha)$. If the observed hZZ coupling agrees with the SM prediction within the 1% accuracy, we may not be able to distinguish the quantum effect from the tree level mixing effect.

The deviation in the hhh coupling can be as large as plus 100% for the mass of h to be around 120 GeV due to the nondecoupling quantum effect of the heavy extra Higgs bosons. This happens even in the SM-like limit, $\sin(\beta - \alpha) \to 1$. Such magnitude of the deviation is larger than the experimental accuracy that is expected to be 10–20% at LCs [6–8], and can be experimentally detected. Therefore, the combination of precise measurements of the hZZ and hhh couplings can be useful to explore the structure of the Higgs sector.

In Sec. II, the form factors of hZZ coupling and hhh coupling are defined, and the SM contribution to them is briefly discussed. In Sec. III, the general feature of the THDM is summarized, and the renormalization scheme of the THDM is defined. The one-loop contributions to the form factors of the hZZ and hhh couplings are calculated in Sec. IV. The analytic properties of the loop corrections are discussed in Sec. V, and the numerical evaluation is shown in Sec. VI. Section VII contains our conclusions. For completeness, we also present the details of our calculation in the appendices.

II. THE hZZ AND hhh COUPLINGS IN THE SM

Before showing the calculation of the form factors in the THDM, it is instructive to discuss the top-quark loop effect on the hZZ and hhh couplings in the SM. One can find a simple example of the nondecoupling effect in the top-quark loop contribution. It is also useful as technical introduction to the calculation in the THDM. In

Appendix A, we show details of the top-quark one-loop contribution to the hZZ and hhh couplings in the SM.

The most general form factors of the hZZ coupling can be written as

$$M^{\mu\nu}_{hZZ} = M^{hZZ}_1 g^{\mu\nu} + M^{hZZ}_2 \frac{p_1^\nu p_2^\mu}{m_Z^2} + M^{hZZ}_3 i\epsilon^{\mu\nu\rho\sigma}\frac{p_{1\rho}p_{2\sigma}}{m_Z^2}, \tag{1}$$

where m_Z is the mass of the Z boson, p_1 and p_2 are the momenta of incoming Z bosons, and we define $g^{\mu\nu} = \mathrm{diag}(1,-1,-1,-1)$ and $\epsilon^{0123} = -1$. The trilinear hhh coupling of the Higgs boson is parametrized by

$$\mathcal{L}_{\mathrm{self}} = +\frac{1}{3!}\Gamma_{hhh}h^3. \tag{2}$$

In the SM, the lowest order contributions to the form factors M^{hZZ}_{1-3} and Γ_{hhh} are given by

$$M_1^{hZZ(\mathrm{tree})} = \frac{2m_Z^2}{v}, \qquad M_2^{hZZ(\mathrm{tree})} = M_3^{hZZ(\mathrm{tree})} = 0, \tag{3}$$

$$\Gamma^{\mathrm{tree}}_{hhh} = -\frac{3m_h^2}{v}, \tag{4}$$

where m_h is the mass of the Higgs boson.

Let us consider the loop contribution of the top quark to these form factors. Details of calculation are presented in Appendix A. From the naive power counting, it is understood that M_1^{hZZ} receives the highest power contribution of the top-quark mass among the form factors of hZZ vertex M_i^{hZZ} $(i = 1-3)$. The leading one-loop contribution of the top quark to the form factor M_1^{hZZ} is calculated as

$$M_1^{hZZ}(p_1^2, p_2^2, p_3^2) = \frac{2m_Z^2}{v}\left[1 - \frac{1}{16\pi^2}\frac{5}{2}\frac{m_t^2}{v^2} \times\left\{1 + \mathcal{O}\left(\frac{m_h^2}{m_t^2}, \frac{p_i^2}{m_t^2}\right)\right\}\right], \tag{5}$$

where m_t is the mass of the top quark, p_i $(i = 1-3)$ represent the momenta of the external lines. The leading top-quark contribution to M_1^{hWW} is the same as that to M_1^{hZZ}, because of the isospin symmetry. Both have the quadratic power contribution of the top-quark mass. On the other hand, the leading contribution of the top quark to the self-coupling constant is calculated [14] as

$$\Gamma_{hhh}(p_1^2, p_2^2, p_3^2) = -\frac{3m_h^2}{v}\left[1 - \frac{1}{16\pi^2}\frac{16m_t^4}{v^2 m_h^2} \times\left\{1 + \mathcal{O}\left(\frac{m_h^2}{m_t^2}, \frac{p_i^2}{m_t^2}\right)\right\}\right]. \tag{6}$$

The top-quark contribution is quartic in mass, so that we expect larger corrections to the hhh coupling than the correction to hZZ vertices by the enhancement factor of $(32/5)m_t^2/m_h^2$ especially when $m_h < m_t$. Equation (6) shows that the leading contribution of the top-quark loop deviates the hhh form factor from the tree level value by about -12% for $m_t = 178$ GeV and $m_h = 120$ GeV. The quartic dependence of the top-quark mass is also reproduced easily in the effective potential method as shown in Appendix A 2.

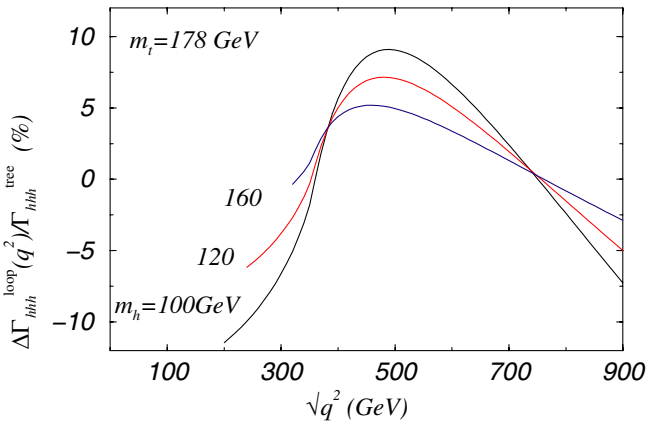

FIG. 1 (color online). The one-loop contribution of the top quark to the effective hhh coupling as a function of $\sqrt{q^2}$, where q^μ is the momentum of the off-shell h boson in $h^* \to hh$. $\Delta\Gamma^{\mathrm{loop}}_{hhh}(q^2)$ is defined by $\Gamma_{hhh}(q^2) - \Gamma^{\mathrm{tree}}_{hhh}$ in the SM.

At the future collider experiment, the hhh coupling will be measured via the double Higgs production processes, where at least one of the three legs of the hhh vertex is off-shell. Thus the momentum dependence in the hhh form factor is important. In Fig. 1, the top-quark loop contribution to the effective hhh coupling $\Gamma_{hhh}(q^2)$ is shown as a function of the invariant mass $(\sqrt{q^2})$ of the virtual h boson for $m_h = 100$, 120, and 160 GeV. $\Gamma_{hhh}(q^2)[\equiv \Gamma_{hhh}(m_h^2, m_h^2, q^2)]$ is evaluated from Eq. (A34) in Appendix A 1. In the small $\sqrt{q^2}$ limit $(\sqrt{q^2} \to 0)$, the correction due to the top-quark loop is negative and approaches to the similar value estimated from Eq. (6). However, such a value of $\sqrt{q^2}$ is lower than the threshold $2m_h$ of the subprocess $h^* \to hh$, and kinematically not allowed. We find that the top-quark loop effect strongly depends on $\sqrt{q^2}$, because the threshold enhancement at $\sqrt{q^2} = 2m_t$ contributes an opposite sign to the quartic mass term contribution. The correction changes the sign when $\sqrt{q^2}$ is somewhere between $2m_h$ and $2m_t$. The enhancement due to the top-pair threshold is maximum at the point just after the threshold of the top-pair production.

III. THE TWO HIGGS DOUBLET MODEL

In this section, we give a brief review of the THDM to make our notation clear and to prepare some tree level formulas, which will be used for the one-loop calculation in the next section. We consider the model with a (softly-

broken) discrete symmetry under the transformation $\Phi_1 \to \Phi_1$ and $\Phi_2 \to -\Phi_2$, where Φ_i are the Higgs isodoublets with hypercharge $\frac{1}{2}$. This discrete symmetry ensures the natural suppression of flavor changing neutral current at tree level. Two types of Yukawa interaction are then possible; i.e., so-called Model I and Model II [21]. In Model I, only Φ_2 is responsible for generating masses for all quarks and charged leptons, whereas in Model II , Φ_1 generates masses of down-type quarks and charged leptons and Φ_2 gives masses of up-type quarks. In our analysis, Model II Yukawa interaction is assumed throughout this paper. Later, we will comment on the case that Model I is considered.

The Higgs potential is given by [21]

$$\begin{aligned} V_{\rm THDM} &= m_1^2|\Phi_1|^2 + m_2^2|\Phi_2|^2 - (m_3^2\Phi_1^\dagger\Phi_2 + \text{h.c.}) \\ &\quad + \frac{\lambda_1}{2}|\Phi_1|^4 + \frac{\lambda_2}{2}|\Phi_2|^4 + \lambda_3|\Phi_1|^2|\Phi_2|^2 \\ &\quad + \lambda_4|\Phi_1^\dagger\Phi_2|^2 + \left\{\frac{\lambda_5}{2}(\Phi_1^\dagger\Phi_2)^2 + \text{h.c.}\right\}, \end{aligned} \tag{7}$$

where m_1^2, m_2^2, and λ_1 to λ_4 are real, while m_3^2 and λ_5 are generally complex. We here assume that there is no CP violation in the Higgs sector, so as to neglect the phases of m_3^2 and λ_5. A nonzero value of m_3^2 indicates that the discrete symmetry is broken softly. Under the assumption, there are eight real parameters in the potential (7). The Higgs sector of the MSSM is a special case of Eq. (7) with Model II Yukawa interaction at tree level.

The Higgs doublets are parametrized as

$$\Phi_i = \begin{bmatrix} w_i^+ \\ \frac{1}{\sqrt{2}}(v_i + h_i + iz_i) \end{bmatrix}, \qquad (i = 1, 2), \tag{8}$$

where v_i $(i = 1, 2)$ are vacuum expectation values that satisfy $\sqrt{v_1^2 + v_2^2} = v \simeq 246$ GeV. We here assume the case with $v_1 v_2 \neq 0$. From the vacuum condition (the stationary condition), we obtain

$$0 = m_3^2 v_2 - m_1^2 v_1 - \frac{1}{2}\lambda_1 v_1^3 - \frac{1}{2}(\lambda_3 + \lambda_4 + \lambda_5) v_1 v_2^2, \tag{9}$$

$$0 = m_3^2 v_1 - m_2^2 v_2 - \frac{1}{2}\lambda_2 v_2^3 - \frac{1}{2}(\lambda_3 + \lambda_4 + \lambda_5) v_1^2 v_2, \tag{10}$$

and the mass parameters m_1^2 and m_2^2 can be eliminated with their degrees of freedom being replaced by those of v_1 and v_2. The mass matrices of the Higgs bosons are diagonalized by introducing the mixing angles β and α. First, we rotate the fields by β as

$$\begin{aligned} \begin{pmatrix} h_1 \\ h_2 \end{pmatrix} &= R(\beta)\begin{pmatrix} \phi_1 \\ \phi_2 \end{pmatrix}, \qquad \begin{pmatrix} z_1 \\ z_2 \end{pmatrix} = R(\beta)\begin{pmatrix} z \\ A \end{pmatrix}, \\ \begin{pmatrix} w_1^+ \\ w_2^+ \end{pmatrix} &= R(\beta)\begin{pmatrix} w^+ \\ H^+ \end{pmatrix}, \end{aligned} \tag{11}$$

$$\text{with } R(\theta) = \begin{pmatrix} \cos\theta & -\sin\theta \\ \sin\theta & \cos\theta \end{pmatrix}. \tag{12}$$

By setting $\tan\beta = v_2/v_1$, the CP-odd and charged states are diagonalized. The Nambu-Goldstone bosons z and $w^\pm$ are massless if the gauge interaction is switched off, and their degrees of freedom are eaten by the longitudinal components of Z and $W^\pm$ bosons when the gauge interaction is turned on. The masses of the physical states A (CP-odd) and $H^\pm$ (charged) are expressed by

$$m_{H^\pm}^2 = M^2 - \frac{1}{2}(\lambda_4 + \lambda_5)v^2, \tag{13}$$

$$m_A^2 = M^2 - \lambda_5 v^2, \tag{14}$$

where v is defined by $v = \sqrt{v_1^2 + v_2^2}$, and M is defined from the remaining degree of freedom of the mass parameter m_3^2 by $M^2 = m_3^2/\sin\beta\cos\beta$. The CP-even states are not yet diagonalized, and the mass matrix for $\phi_{1,2}$ is given by M_{ij}^2, where

$$M_{11}^2 = (\lambda_1\cos^4\beta + \lambda_2\sin^4\beta + 2\lambda\cos^2\beta\sin^2\beta)v^2, \tag{15}$$

$$M_{12}^2 = (-\lambda_1\cos^2\beta + \lambda_2\sin^2\beta + \lambda\cos2\beta)\cos\beta\sin\beta v^2, \tag{16}$$

$$M_{22}^2 = M^2 + \frac{1}{8}(\lambda_1 + \lambda_2 - 2\lambda)(1 - \cos4\beta)v^2, \tag{17}$$

with $\lambda = \lambda_3 + \lambda_4 + \lambda_5$. The diagonalized CP-even states (H, h) are obtained from (ϕ_1, ϕ_2) by the rotation with the angle $(\alpha - \beta)$ as

$$\begin{pmatrix} \phi_1 \\ \phi_2 \end{pmatrix} = R(\alpha - \beta)\begin{pmatrix} H \\ h \end{pmatrix}. \tag{18}$$

The mixing angle $(\alpha - \beta)$ and the mass eigenstates are determined as

$$\tan2(\alpha - \beta) = \frac{2M_{12}^2}{M_{11}^2 - M_{22}^2}, \tag{19}$$

and

$$\begin{aligned} m_H^2 &= \cos^2(\alpha - \beta)M_{11}^2 + \sin2(\alpha - \beta)M_{12}^2 \\ &\quad + \sin^2(\alpha - \beta)M_{22}^2, \end{aligned} \tag{20}$$

$$\begin{aligned} m_h^2 &= \sin^2(\alpha - \beta)M_{11}^2 - \sin2(\alpha - \beta)M_{12}^2 \\ &\quad + \cos^2(\alpha - \beta)M_{22}^2, \end{aligned} \tag{21}$$

respectively. The two physical CP-even fields h and H are

defined so as to satisfy $m_h \lesssim m_H$. Among M_{ij}^2, only M_{22}^2 includes the dimensionful parameter M. In the limit of $M^2 \to \infty$, we have $\tan 2(\alpha - \beta) \to 0$. The angle α is chosen such that $m_h^2 \to M_{11}^2$, $m_H^2 \to M^2$, and $\sin(\alpha - \beta) \to -1$ are satisfied in the limit $M^2 \to +\infty$.[1]

We note that the masses of the heavier Higgs bosons (H, $H^\pm$ and A) take the form as

$$m_\Phi^2 = M^2 + \lambda_i v^2[+\mathcal{O}(v^4/M^2)], \tag{22}$$

where Φ represents H, H^+ or A and λ_i is a linear combination of λ_1-λ_5. When $M^2 \gg \lambda_i v^2$, the mass m_Φ^2 is determined by the soft-breaking scale of the discrete symmetry M^2, and is independent of λ_i. In this case, the effective theory below M is described by one Higgs doublet, and all the tree level couplings related to the lightest Higgs boson h approach to the SM value. Furthermore, the loop effects of Φ vanish in the large mass limit ($m_\Phi \to \infty$) because of the decoupling theorem [40]. The MSSM Higgs sector corresponds to this case, because λ_i is fixed to be $\mathcal{O}(g^2)$ so that large mass of Φ is possible only by large values of M. On the contrary, when M^2 is limited to be at the weak scale ($M^2 \lesssim \lambda_i v^2$) a large value of m_Φ is realized by taking λ_i to be large; i.e., the strong coupling regime. In this case, the squared mass of Φ is effectively proportional to λ_i, so that the decoupling theorem does not apply. Then, we expect a powerlike contribution of m_Φ in the radiative correction. We call such an effect the nondecoupling effect of Φ [29–33]. Similar nondecoupling effect appears in considering the top-quark loop contributions in the SM. Although we expect large loop effects in this case, theoretical and experimental constraints must be considered. For instance, too large λ_i leads to the breakdown of validity of perturbation calculation [34–36]. Furthermore, the low energy precision data also impose important constraints on the model parameters [41]. Later, in our evaluation of the one-loop form factors, we shall take into account these constraints.

The parameters of the Higgs potential are m_1^2-m_3^2 and λ_1-λ_5. They can be rewritten by eight "physical" parameters; i.e., four Higgs mass parameters $m_h, m_H, m_A, m_{H^\pm}$, two mixing angles α, β, the vacuum expectation value v, and the soft-breaking scale of the discrete symmetry M. The quartic coupling constants can be expressed in terms of these physical parameters as

$$\lambda_1 = \frac{1}{v^2\cos^2\beta}(-\sin^2\beta M^2 + \sin^2\alpha m_h^2 + \cos^2\alpha m_H^2), \tag{23}$$

$$\lambda_2 = \frac{1}{v^2\sin^2\beta}(-\cos^2\beta M^2 + \cos^2\alpha m_h^2 + \sin^2\alpha m_H^2), \tag{24}$$

$$\lambda_3 = -\frac{M^2}{v^2} + 2\frac{m_{H^\pm}^2}{v^2} + \frac{1}{v^2}\frac{\sin 2\alpha}{\sin 2\beta}(m_H^2 - m_h^2), \tag{25}$$

$$\lambda_4 = \frac{1}{v^2}(M^2 + m_A^2 - 2m_{H^\pm}^2), \tag{26}$$

$$\lambda_5 = \frac{1}{v^2}(M^2 - m_A^2). \tag{27}$$

IV. ONE-LOOP CORRECTION TO *hZZ* AND *hhh* IN THE THDM

We here discuss our scheme for calculating the one-loop corrections to the form factors of hZZ and hhh in the THDM. As we are interested in the Higgs nondecoupling effects, we neglect the loop contributions of the gauge bosons in the calculation. This procedure is justified by adopting Landau gauge, where the effect of the gauge bosons and that of the Higgs bosons can be treated separately. The renormalization is performed in the on-shell scheme for physical mass parameters and mixing angles.

First, we renormalize the three SM input parameters m_W, m_Z, and G_F ($= \frac{1}{\sqrt{2}v^2}$). The counterterms of gauge boson masses (δm_W^2, δm_Z^2) and the wave function renormalization factors (δZ_W, δZ_Z) are obtained by calculating the transverse part $\Pi_T^{VV}(p^2)$ of the two-point function:

$$\Pi_{\mu\nu}^{VV}(p^2) = \left(-g_{\mu\nu} + \frac{p_\mu p_\nu}{p^2}\right)\Pi_T^{VV}(p^2) + \frac{p_\mu p_\nu}{p^2}\Pi_L^{VV}(p^2), \tag{28}$$

where $VV = WW$ or ZZ. In the on-shell renormalization scheme, we obtain

$$\delta m_V^2 = \mathrm{Re}\Pi_T^{VV(1\mathrm{PI})}(m_V^2), \tag{29}$$

$$\delta Z_V = -\frac{\partial}{\partial p^2}\mathrm{Re}\Pi_T^{VV(1\mathrm{PI})}(p^2)\Big|_{p^2=m_V^2}. \tag{30}$$

[1] Equivalently, we may rotate the CP-even fields from (h_1, h_2) to (H, h) by the angle α directly. Then we obtain

$$\tan 2\alpha = \frac{\{M^2 - (\lambda_3 + \lambda_4 + \lambda_5)v^2\}\sin 2\beta}{(M^2 - \lambda_1 v^2)\cos^2\beta - (M^2 - \lambda_2 v^2)\sin^2\beta},$$

and

$$m_H^2 = M^2\sin^2(\alpha - \beta) + \left(\lambda_1\cos^2\alpha\cos^2\beta + \lambda_2\sin^2\alpha\sin^2\beta + \frac{1}{2}\lambda\sin 2\alpha\sin 2\beta\right)v^2,$$

$$m_h^2 = M^2\cos^2(\alpha - \beta) + \left(\lambda_1\sin^2\alpha\cos^2\beta + \lambda_2\cos^2\alpha\sin^2\beta - \frac{1}{2}\lambda\sin 2\alpha\sin 2\beta\right)v^2.$$

One can easily check that the above two expressions for m_h and m_H are equivalent.

The renormalization for the vacuum expectation value δv ($v \to v + \delta v$) is defined by

$$\frac{\delta v}{v} = \frac{1}{2}\frac{1}{m_W^2}\Pi_T^{WW}(0) + (\text{vertex and box corrections}). \tag{31}$$

When neglecting the vertex and box contributions, which are $\mathcal{O}(\alpha_{EM})$, $\delta v/v$ can be expressed solely by the oblique correction $\Pi_T^{WW}(0)$.[2]

Next, let us define the renormalization scheme for the Higgs sector. In addition to v, the bare parameters of the Higgs potential are $m_h^2, m_H^2, m_A^2, m_{H^\pm}^2, \alpha, \beta, M^2, T_h, T_H$, where T_h and T_H are tadpoles of h and H, respectively. The tadpole parameters are fixed by the stationary condition at each order of perturbation. At the tree level, we set $T_h = T_H = 0$, while at one-loop level T_h and T_H are chosen to make the renormalized one-point functions for h and H to be zero. They are expressed in terms of the Lagrangian parameters as

$$T_H = T_1\cos\alpha + T_2\sin\alpha, \qquad T_h = -T_1\sin\alpha + T_2\cos\alpha, \tag{32}$$

with

$$T_1 = m_3^2 v_2 - m_1^2 v_1 - \frac{1}{2}\lambda_1 v_1^3 - \frac{1}{2}(\lambda_3+\lambda_4+\lambda_5) v_1 v_2^2, \tag{33}$$

$$T_2 = m_3^2 v_1 - m_2^2 v_2 - \frac{1}{2}\lambda_2 v_2^3 - \frac{1}{2}(\lambda_3+\lambda_4+\lambda_5) v_1^2 v_2. \tag{34}$$

The renormalized parameters are defined by shifting the bare parameters as

$$T_{h,H} \to 0 + \delta T_{h,H}, \tag{35}$$

$$m_{\phi_i}^2 \to m_{\phi_i}^2 + \delta m_{\phi_i}^2, \tag{36}$$

$$\alpha \to \alpha + \delta\alpha, \tag{37}$$

$$\beta \to \beta + \delta\beta, \tag{38}$$

$$M^2 \to M^2 + \delta M^2, \tag{39}$$

where ϕ_i represents H, h, A, and $H^\pm$. The introduction of the wave function renormalization factors for the Higgs bosons is rather complicated because the mixing between scalar bosons with the same quantum number should be taken into account. According to the method explained in Appendix C, we define

$$\begin{bmatrix} H \\ h \end{bmatrix} \to \begin{bmatrix} 1+\frac{1}{2}\delta Z_H & \delta\alpha + \delta C_h \\ -\delta\alpha + \delta C_h & 1+\frac{1}{2}\delta Z_h \end{bmatrix}\begin{bmatrix} H \\ h \end{bmatrix}, \tag{40}$$

where δZ_h (δZ_H) is the wave function factor of h (H). Similarly, for the CP-odd scalar bosons and the charged scalar bosons we define

$$\begin{bmatrix} z \\ A \end{bmatrix} \to \begin{bmatrix} 1+\frac{1}{2}\delta Z_z & \delta\beta + \delta C_A \\ -\delta\beta + \delta C_A & 1+\frac{1}{2}\delta Z_A \end{bmatrix}\begin{bmatrix} z \\ A \end{bmatrix}, \tag{41}$$

and

$$\begin{bmatrix} w^\pm \\ H^\pm \end{bmatrix} \to \begin{bmatrix} 1+\frac{1}{2}\delta Z_{w^\pm} & \delta\beta + \delta C_{H^+} \\ -\delta\beta + \delta C_{H^+} & 1+\frac{1}{2}\delta Z_{H^\pm} \end{bmatrix}\begin{bmatrix} w^\pm \\ H^\pm \end{bmatrix}, \tag{42}$$

respectively, where δZ_A, $\delta Z_{H^\pm}$ are the wave function renormalization factors for the physical CP-odd and charged Higgs bosons A and $H^\pm$. In addition, we introduced the "wave function" factors δZ_z and δZ_w for the Nambu-Goldstone bosons z and $w^\pm$, which are massless in the Landau gauge. However, δZ_z and δZ_w will not be used in our calculation.

There are 16 counterterm parameters ($\delta T_{h,H}$, $\delta m_{\phi_i}^2$, δZ_{ϕ_i}, $\delta\alpha$, $\delta\beta$, δC_h, δC_A, δC_{H^+}, and δM^2), where $\phi_i = H, h, A$ and $H^\pm$, and δC_h, δC_A, and δC_{H^+} are defined via Eqs. (40)–(42). The first 15 of them are determined by imposing the renormalization condition to the one- and two-point functions. The conditions are shown below in order.

The tadpole condition requires that the renormalized one-point functions for h and H must satisfy

$$\Gamma_h = 0, \qquad \Gamma_H = 0, \tag{43}$$

with $\Gamma_{h,H} = T^{1\text{PI}} + \delta T_{h,H}$. Thus,

$$\delta T_h = -T_h^{1\text{PI}}, \qquad \delta T_H = -T_H^{1\text{PI}}, \tag{44}$$

where $T_{h,H}^{1\text{PI}}$ are the contributions of one-particle-irreducible (1PI) diagrams. The explicit expressions of the contributions to $T_{h,H}^{1\text{PI}}$ in the THDM are given in Appendix B.

The relevant renormalized two-point functions for $h, H, A, H^\pm$ can be expressed as

$$\Gamma_{hh}(p^2) = \Pi_{hh}^{1\text{PI}}(p^2) + \left\{(p^2 - m_h^2)(1+\delta Z_h) - \delta m_h^2 + \frac{\sin^2\alpha}{\cos\beta}\frac{\delta T_1}{v} + \frac{\cos^2\alpha}{\sin\beta}\frac{\delta T_2}{v}\right\}, \tag{45}$$

$$\Gamma_{HH}(p^2) = \Pi_{HH}^{1\text{PI}}(p^2) + \left\{(p^2 - m_H^2)(1+\delta Z_H) - \delta m_H^2 + \frac{\cos^2\alpha}{\cos\beta}\frac{\delta T_1}{v} + \frac{\sin^2\alpha}{\sin\beta}\frac{\delta T_2}{v}\right\}, \tag{46}$$

[2]It is straightforward to see the difference from the other renormalization schemes in which the SM inputs are taken as (α_{EM}, m_Z, G_F) or (m_W, m_Z, α_{EM}). The difference is of order α_{EM} which is neglected in the present calculation.

$$\Gamma_{AA}(p^2) = \Pi^{\rm 1PI}_{AA}(p^2) + \Big\{(p^2 - m_A^2)(1 + \delta Z_A) - \delta m_A^2 + \left(\frac{\sin^2\beta}{\cos\beta} - \cos\beta + \frac{1}{\cos\beta}\right)\frac{\delta T_1}{2v} + \left(\frac{\cos^2\beta}{\sin\beta} - \sin\beta + \frac{1}{\sin\beta}\right)\frac{\delta T_2}{2v}\Big\}, \quad (47)$$

$$\Gamma_{H^+H^-}(p^2) = \Pi^{\rm 1PI}_{H^+H^-}(p^2) + \Big\{(p^2 - m_{H^\pm}^2)(1 + \delta Z_{H^\pm}) - \delta m_{H^\pm}^2 + \left(\frac{\sin^2\beta}{\cos\beta} - \cos\beta + \frac{1}{\cos\beta}\right)\frac{\delta T_1}{2v} + \left(\frac{\cos^2\beta}{\sin\beta} - \sin\beta + \frac{1}{\sin\beta}\right)\frac{\delta T_2}{2v}\Big\}, \quad (48)$$

where $\Pi^{\rm 1PI}_{\phi\phi}(p^2)$ are the 1PI diagram contributions to the self-energies. Their expressions and those of δT_1 and δT_2 are summarized in Appendix B.

By imposing the on-shell conditions

$$\mathrm{Re}\Gamma_{\phi_i\phi_i}(m^2_{\phi_i}) = 0, \qquad \frac{\partial}{\partial p^2}\mathrm{Re}\Gamma_{\phi_i\phi_i}(p^2)\Big|_{p^2=m^2_{\phi_i}} = 1, \quad (49)$$

where ϕ_i represents h,H,A, and $H^\pm$, we determine δm_h^2, δm_H^2, δm_A^2, $\delta m_{H^\pm}^2$, δZ_h, δZ_H, δZ_A, and $\delta Z_{H^\pm}$.

The condition that there is no mixing between CP-even scalar bosons h and H on each mass shell; i.e.,

$$\Gamma_{hH}(m_h^2) = 0, \qquad \Gamma_{hH}(m_H^2) = 0, \quad (50)$$

determines $\delta\alpha$ and δC_h, where

$$\Gamma_{hH}(p^2) = \tilde{\Pi}_{hH}(p^2) + (2p^2 - m_h^2 - m_H^2)\delta C_h - (m_H^2 - m_h^2)\delta\alpha, \quad (51)$$

with

$$\tilde{\Pi}_{hH}(p^2) = \Pi^{\rm 1PI}_{hH}(p^2) + \cos\alpha\sin\alpha\left(-\frac{1}{\cos\beta}\frac{\delta T_1}{v} + \frac{1}{\sin\beta}\frac{\delta T_2}{v}\right). \quad (52)$$

Hence, we obtain

$$\delta\alpha = +\frac{1}{2}\frac{1}{m_H^2 - m_h^2}\{\tilde{\Pi}_{hH}(m_H^2) + \tilde{\Pi}_{hH}(m_h^2)\}, \quad (53)$$

$$\delta C_h = -\frac{1}{2}\frac{1}{m_H^2 - m_h^2}\{\tilde{\Pi}_{hH}(m_H^2) - \tilde{\Pi}_{hH}(m_h^2)\}. \quad (54)$$

The expression of the 1PI diagrams $\tilde{\Pi}_{hH}(p^2)$ can be obtained from those of Π_{hH}, δT_1, and δT_2 in Appendix B.

The parameters $\delta\beta$, δC_A, and δC_{H^+} are determined by the conditions for the two-point functions of z-A and $w^\pm$-$H^\pm$ mixings. For the CP-odd sector, we require

$$\Gamma_{zA}(0) = 0, \quad (55)$$

$$\Gamma_{zA}(m_A^2) = 0, \quad (56)$$

where

$$\Gamma_{zA}(p^2) = \tilde{\Pi}_{zA}(p^2) + (2p^2 - m_A^2)\delta C_A + m_A^2\delta\beta, \quad (57)$$

with

$$\tilde{\Pi}_{zA}(p^2) = \Pi^{\rm 1PI}_{zA}(p^2) - \sin\beta\frac{\delta T_1}{v} + \cos\beta\frac{\delta T_2}{v}. \quad (58)$$

Because of the Nambu-Goldstone theorem, $\tilde{\Pi}_{zA}(0) = 0$ is ensured, so that we obtain, from Eqs. (55) and (56),

$$\delta C_A = \delta\beta = -\frac{1}{2m_A^2}\tilde{\Pi}_{zA}(m_A^2). \quad (59)$$

For the charged sector, from the condition

$$\Gamma_{w^\pm H^\mp}(0) = 0, \quad (60)$$

where

$$\Gamma_{w^\pm H^\mp}(p^2) = \tilde{\Pi}_{w^\pm H^\mp}(p^2) + (2p^2 - m_{H^\pm}^2)\delta C_{H^+} + m_{H^\pm}^2\delta\beta, \quad (61)$$

with

$$\tilde{\Pi}_{w^\pm H^\mp}(p^2) = \tilde{\Pi}^{\rm 1PI}_{w^\pm H^\mp}(p^2) - \sin\beta\frac{\delta T_1}{v} + \cos\beta\frac{\delta T_2}{v}, \quad (62)$$

we obtain

$$\delta C_{H^+} = \delta\beta. \quad (63)$$

We note that due to the Ward-Takahashi identity, the condition (56) is equivalent to the following condition on the mixing between the gauge boson and the Higgs boson:

$$\Gamma_{ZA}(m_A^2) = 0, \quad (64)$$

where the two-point function of ZA is written as

$$\Gamma^\mu_{ZA}(p^2) = -ip^\mu\Gamma_{ZA}(p^2), \quad (65)$$

and the form factor $\Gamma_{ZA}(p^2)$ is expressed as

$$\Gamma_{ZA}(p^2) = (\delta\beta + \delta C_A)m_Z + \Gamma^{\rm 1PI}_{ZA}(p^2). \quad (66)$$

In the above equation, the counterterm parameter $(\delta\beta + \delta C_A)$ comes from the Higgs kinematic terms of the Lagrangian as the consequence of the shift of the parameters:

$$\mathcal{L} = m_Z(\partial_\mu z)Z^\mu \to +(\delta\beta + \delta C_A)m_Z(\partial_\mu A)Z^\mu + \cdots. \quad (67)$$

With the expressions of $\Gamma^{\rm 1PI}_{ZA}(p^2)$ and $\Gamma^{\rm 1PI}_{zA}(p^2)$ presented in Appendix B, one can explicitly check the equivalence of the conditions of Eqs. (56) and (64). Similarly, instead of the condition (56), the alternative condition

$$\Gamma_{w^\pm H^\mp}(m_{H^\pm}^2) = 0 \quad (68)$$

may be used to determine $\delta\beta$. In this case, $\delta\beta$ (let us denote it as $\delta\beta'$) is given by

$$\delta\beta'(=\delta C'_{H^+}=\delta C'_A)=-\frac{1}{2m^2_{H^\pm}}\tilde{\Pi}_{w^\pm H^\mp}(m^2_{H^\pm}). \quad (69)$$

It is easy to check that the difference between $\delta\beta$ and $\delta\beta'$ is finite. This finite difference is due to different choice of renormalization prescription in loop calculations. In this paper, we adopt $\delta\beta$ determined from Eqs. (55) and (56).

We have determined all the renormalization parameters but δM^2 of the Higgs sector by applying the renormalization conditions to various one- and two-point functions. However, the renormalization of M^2 has to be discussed in the context of three-point functions. Below, we consider the renormalization calculation for the three-point hZZ and hhh vertices.

The tree level hZZ coupling can be read out from the kinematic term of the Lagrangian:

$$\mathcal{L}_{hZZ}=+\frac{m^2_Z}{v}\sin(\beta-\alpha)g_{\mu\nu}Z^\mu Z^\nu h + \frac{m^2_Z}{v}\cos(\beta-\alpha)g_{\mu\nu}Z^\mu Z^\nu H. \quad (70)$$

In terms of the general form factors of the hZZ coupling, cf. Eq. (1), we get

$$M_1^{hZZ(\text{tree})}=\frac{2m^2_Z}{v}\sin(\beta-\alpha), \qquad M_2^{hZZ(\text{tree})}=M_3^{hZZ(\text{tree})}=0. \quad (71)$$

On the other hand, the tree level coupling constants of hhh and hhH are given from the Higgs potential. By using the mass relations of Eqs. (23)–(27), each coupling constant can be expressed in terms of Higgs boson masses and mixing angles:

$$\lambda_{hhh}=\frac{-1}{4v\sin2\beta}[\{\cos(3\alpha-\beta)+3\cos(\alpha+\beta)\}m_h^2 - 4\cos^2(\alpha-\beta)\cos(\alpha+\beta)M^2], \quad (72)$$

$$\lambda_{hhH}=\frac{-1}{2v\sin2\beta}\{\cos(\alpha-\beta)\sin2\alpha(2m_h^2+m_H^2) - \cos(\alpha-\beta)(3\sin2\alpha-\sin2\beta)M^2\}. \quad (73)$$

The tree level form factor for the hhh coupling, $\Gamma^{(\text{tree})}_{hhh}$, is thus given by

$$\Gamma^{(\text{tree})}_{hhh}=3!\lambda_{hhh}. \quad (74)$$

Note that in the SM-like limit ($\alpha=\beta-\pi/2$), the form factors of hZZ and hhh couplings take the same form as in the SM:

$$M_1^{hZZ(\text{tree})}=\frac{2m^2_Z}{v}, \qquad M_2^{hZZ(\text{tree})}=M_3^{hZZ(\text{tree})}=0, \quad (75)$$

$$\Gamma^{(\text{tree})}_{hhh}=-\frac{3m_h^2}{v}, \quad (76)$$

while the heavier Higgs boson H does not couple to the gauge bosons and also $\lambda_{hhH}=0$.

Now, we discuss the renormalized vertices of hZZ and hhh. From the kinematic term of the Higgs sector, we obtain the counterterms to the form factors of the hZZ vertex as follows.

$$\begin{aligned}\mathcal{L}_{hZZ}&=-\frac{m^2_Z}{v}\sin(\alpha-\beta)g_{\mu\nu}Z^\mu Z^\nu h + \frac{m^2_Z}{v}\cos(\alpha-\beta)g_{\mu\nu}Z^\mu Z^\nu H \\ &\to -\frac{m^2_Z}{v}\left\{\sin(\alpha-\beta)\left(1+\frac{\delta m^2_Z}{m^2_Z}-\frac{\delta v}{v}+\delta Z_Z + \frac{1}{2}\delta Z_h\right)+\cos(\alpha-\beta)(-\delta\beta-\delta C_h)\right\} \\ &\quad\times g_{\mu\nu}Z^\mu Z^\nu h+\cdots. \end{aligned} \quad (77)$$

Thus, we obtain the counterterms for the hZZ form factors as

$$\delta M_1^{hZZ}=-\frac{2m^2_Z}{v}\left\{\sin(\alpha-\beta)\left(\frac{\delta m^2_Z}{m^2_Z}-\frac{\delta v}{v}+\delta Z_Z + \frac{1}{2}\delta Z_h\right)+\cos(\alpha-\beta)(-\delta\beta-\delta C_h)\right\}, \quad (78)$$

$$\delta M_2^{hZZ}=\delta M_3^{hZZ}=0. \quad (79)$$

The counterterm for the hhh vertex is obtained from the shifting of the bare hhh coupling $\delta\lambda_{hhh}$ and the wave function and mixing renormalization of the hhh and hhH vertices as

$$\lambda_{hhh}\to\lambda_{hhh}+\delta\lambda_{hhh}, \quad (80)$$

$$hhh\to\left\{\left(1+\frac{1}{2}\delta Z_h\right)h+\cdots\right\}^3\to\left(1+\frac{3}{2}\delta Z_h\right)h^3+\cdots, \quad (81)$$

$$hhH\to\left\{\left(1+\frac{1}{2}\delta Z_h\right)h+\cdots\right\}^2\{(\delta\alpha+\delta C_h)h+\cdots\} \to(\delta\alpha+\delta C_h)h^3+\cdots. \quad (82)$$

Thus, the counterterm for the Γ_{hhh} is obtained as

$$\delta\Gamma_{hhh}=3!\left\{\delta\lambda_{hhh}+\frac{3}{2}\lambda_{hhh}\delta Z_h+\lambda_{hhH}(\delta\alpha+\delta C_h)\right\} \quad (83)$$

$$=3!\lambda_{hhh}\left(\frac{3}{2}\delta Z_h-\frac{\delta v}{v}\right)+3!\lambda_{hhH}\delta C_h+C_1\delta m_h^2 + C_2\delta\alpha+C_3\delta\beta+C_4\delta M^2, \quad (84)$$

where

$$C_1 = \frac{-1}{4v\sin 2\beta}\{\cos(3\alpha-\beta)+3\cos(\alpha+\beta)\}, \quad (85)$$

$$C_2 = \frac{-1}{2v\sin 2\beta}\cos(\alpha-\beta)\sin 2\alpha(m_H^2-m_h^2), \quad (86)$$

$$C_3 = \frac{\cos(\alpha-\beta)}{4v\sin^2 2\beta}[\{4+\cos 2(\alpha-\beta)+3\cos 2(\alpha+\beta)\}m_h^2 - \{5+\cos 2(\alpha-\beta)-\cos 4\beta + 3\cos 2(\alpha+\beta)\}M^2], \quad (87)$$

$$C_4 = \frac{1}{v\sin 2\beta}\cos^2(\alpha-\beta)\cos(\alpha+\beta). \quad (88)$$

Up to now we have not explicitly discussed the renormalization condition to determine the counterterm of the soft-breaking mass, δM^2. We chose to fix this parameter in the minimal subtraction method. Namely, we require the condition that the remaining divergent term (proportional to Δ) in the hhh vertex is canceled by the counterterm δM^2. In the present model, $\delta M^2/M^2$ is found to be

$$\frac{\delta M^2}{M^2} = \frac{1}{16\pi^2 v^2}\left\{2N_c(m_t^2\cot^2\beta + m_b^2\tan^2\beta) + 4M^2 - 2m_{H^\pm}^2 - m_A^2 + \frac{\sin 2\alpha}{\sin 2\beta}(m_H^2-m_h^2)\right\}\Delta, \quad (89)$$

where $\Delta = 1/\epsilon + \ln\mu^2$ with $D = 4-2\epsilon$.

Finally, the renormalized form factors for hZZ and hhh couplings are calculated by

$$M_i^{hZZ}(p_1^2, p_2^2, q^2) = M_i^{hZZ(\mathrm{tree})} + M_i^{hZZ(1\mathrm{PI})}(p_1^2, p_2^2, q^2) + \delta M_i^{hZZ}, \qquad (i = 1-3), \quad (90)$$

$$\Gamma_{hhh}(p_1^2, p_2^2, q^2) = \Gamma_{hhh}^{\mathrm{tree}} + \Gamma_{hhh}^{1\mathrm{PI}}(p_1^2, p_2^2, q^2) + \delta\Gamma_{hhh}, \quad (91)$$

where the momentum q^μ in Eq. (90) is that of the external Higgs boson line, and all the counterterms are completely determined by the renormalization conditions in Eqs. (43), (49), (50), (55), (56), (60), and (89). All the explicit results for the 1PI diagrams which contribute to the form factors are summarized in Appendix B.

V. LARGE MASS EXPRESSION IN THE SM-LIKE REGIME

The renormalized coupling constants hZZ and hhh are evaluated by the formulas given in Eqs. (90) and (91). The deviation from the SM predictions can occur due to two sources: the mixing effect which appears in the tree level, and the quantum correction effect due to the loop contribution of the extra Higgs bosons. If the mixing between the two CP-even Higgs bosons is large (e.g., $\sin^2(\alpha-\beta)\sim 0.3-0.7$), the hZZ form factor M_1^{hZZ} in the THDM significantly differs from the SM prediction already at tree level by the factor of $\sin(\beta-\alpha)$; cf. Eq. (71). In such a case, we may be able to obtain an indirect but explicit evidence of extended Higgs sectors at the LHC or at the early stage of the LC experiments.

On the other hand, the hZZ coupling may be close to the SM prediction; i.e., in the SM-like regime [42] where $\sin^2(\alpha-\beta)\simeq 1$. Define $x = \beta-\alpha-\pi/2$. As $x \ll 1$, the tree level hZZ and hhh couplings can be expressed as follows:

$$M_1^{hZZ(\mathrm{tree})} = \frac{2m_Z^2}{v}\left\{1-\frac{1}{2}x^2+\mathcal{O}(x^4)\right\}, \quad (92)$$

$$\Gamma_{hhh}^{(\mathrm{tree})} = -\frac{3m_h^2}{v}\left\{1+\frac{3}{2}\left(1-\frac{4M^2}{3m_h^2}\right)x^2+\mathcal{O}(x^3)\right\}. \quad (93)$$

In the limit of $x\to 0$, the mixing effect vanishes and the hZZ and hhh couplings coincide with the SM formulas. From Eq. (93), we find that in the SM-like regime the hhh coupling constant is reduced from the SM value as long as $M^2 > 3m_h^2/4$. Keeping only the leading one-loop contributions of the heavier Higgs bosons and the top quark, the expressions for the one-loop corrected hZZ and hhh couplings are given in the SM-like regime ($x \ll 1$) as

$$M_1^{hZZ} = \frac{2m_Z^2}{v}\left\{1-\frac{1}{2}x^2+\frac{1}{64\pi^2v^2}(m_H^2+m_A^2+2m_{H^\pm}^2) - \frac{m_H^2}{96\pi^2v^2}\left(1-\frac{M^2}{m_H^2}\right)^2 - \frac{m_A^2}{96\pi^2v^2}\left(1-\frac{M^2}{m_A^2}\right)^2 - \frac{m_{H^\pm}^2}{48\pi^2v^2}\left(1-\frac{M^2}{m_{H^\pm}^2}\right)^2 - \frac{5N_{c_t}m_t^2}{96\pi^2v^2} + \mathcal{O}\left(x^4, \frac{p_i^2}{v^2}, \frac{m_h^2}{v^2}\right)\right\}, \quad (94)$$

$$\Gamma_{hhh} = -\frac{3m_h^2}{v}\left\{1+\frac{3}{2}\left(1-\frac{4M^2}{3m_h^2}\right)x^2+\frac{m_H^4}{12\pi^2m_h^2v^2}\times\left(1-\frac{M^2}{m_H^2}\right)^3+\frac{m_A^4}{12\pi^2m_h^2v^2}\left(1-\frac{M^2}{m_A^2}\right)^3 + \frac{m_{H^\pm}^4}{6\pi^2m_h^2v^2}\left(1-\frac{M^2}{m_{H^\pm}^2}\right)^3-\frac{N_{c_t}m_t^4}{3\pi^2m_h^2v^2} + \mathcal{O}\left(x^3, \frac{p_i^2m_\Phi^2}{v^2m_h^2}, \frac{m_\Phi^2}{v^2}, \frac{p_i^2m_t^2}{v^2m_h^2}, \frac{m_t^2}{v^2}\right)\right\}, \quad (95)$$

where m_Φ represents the masses of the heavier Higgs

bosons H, A, and $H^{\pm}$.[3] As expected, there are quartic power terms of the heavier Higgs boson masses in Γ_{hhh}. The difference from the top-mass contribution is the suppression factor of $(1 - M^2/m_\Phi^2)^3$ and the sign. The large correction occurs in the case of small M^2. The largest corresponds to the limit of $M^2 \to 0$. In this case, a greater positive deviation from the SM prediction is obtained for a larger m_Φ. However, since m_Φ^2 is originated from the electroweak symmetry breaking and is proportional to λ_i, a too large value of m_Φ^2 is forbidden by the requirement of the perturbative unitarity [34]. Furthermore, the direction of the deviation induced by the heavy Higgs boson (bosonic) loops is opposite to that by the top-quark (fermionic) loops.

$$\left(\frac{\Delta g_{hZZ}^{\mathrm{THDM}}}{g_{hZZ}^{\mathrm{SM}}}\right)(q^2) = \frac{M_1^{hZZ(\mathrm{THDM})}(m_h^2, m_Z^2, q^2) - M_1^{hZZ(\mathrm{SM})}(m_h^2, m_Z^2, q^2)}{M_1^{hZZ(\mathrm{SM})}(m_h^2, m_Z^2, q^2)}, \tag{96}$$

$$\left(\frac{\Delta \lambda_{hhh}^{\mathrm{THDM}}}{\lambda_{hhh}^{\mathrm{SM}}}\right)(q^2) = \frac{\Gamma_{hhh}^{\mathrm{THDM}}(m_h^2, m_h^2, q^2) - \Gamma_{hhh}^{\mathrm{SM}}(m_h^2, m_h^2, q^2)}{\Gamma_{hhh}^{\mathrm{SM}}(m_h^2, m_h^2, q^2)}, \tag{97}$$

where the SM form factors $M_1^{hZZ(\mathrm{SM})}(p_1^2, p_2^2, q^2)$ and $\Gamma_{hhh}^{\mathrm{SM}}(p_1^2, p_2^2, q^2)$ are evaluated by using Eqs. (A33) and (A34), and those of the THDM, $M_1^{hZZ(\mathrm{THDM})}(p_1^2, p_2^2, q^2)$ and $\Gamma_{hhh}^{\mathrm{SM}}(p_1^2, p_2^2, q^2)$, are given by Eqs. (90) and (91). In the following numerical analysis, we fix $\sqrt{q^2} = 2m_h$ except for in Fig. 4. We show the momentum dependence of the deviation in the hhh form factor in Fig. 4. Throughout this section, the mass of the top quark is set to be $m_t = 175$ GeV.

A. The SM-like limit

First, we show the results in the SM-like limit [$\sin^2(\alpha - \beta) = 1$ or $x \to 0$ in Eqs. (94) and (95)], where the tree level expressions coincide with the SM ones; cf. Eqs. (92) and (93). In this case, the contributions to $\Delta g_{hZZ}^{\mathrm{THDM}}$ and $\Delta \lambda_{hhh}^{\mathrm{THDM}}$ only come from radiative corrections. The form factor M_1^{hZZ} receives the one-loop effect of $\mathcal{O}[m_\Phi^2/(16\pi^2 v^2)]$ due to the heavy Higgs boson Φ ($\Phi = H$, A, and $H^{\pm}$) with the suppression factor $(1 - M^2/m_\Phi^2)^2$. When $M = 0$, where the nondecoupling loop effect is maximal, the magnitude of the deviation $\Delta g_{hZZ}^{\mathrm{THDM}}/g_{hZZ}^{\mathrm{SM}}$ becomes typically at most $\mathcal{O}(1)\%$. On the other hand, the loop effect for the hhh coupling is $\mathcal{O}[m_\Phi^4/(16\pi^2 v^2 m_h^2)]$ with the suppression factor $(1 - M^2/m_\Phi^2)^3$. The magnitude is larger than that for the hZZ coupling by the enhancement factor of m_Φ^2/m_h^2 [13,14]. In Fig. 2, the one-loop contribution of the heavy Higgs bosons to the hhh coupling is shown for $m_h = 100$, 120, and 160 GeV as a function of m_Φ, where $m_\Phi \equiv m_H = m_A = m_{H^{\pm}}$, by assuming $\sin^2(\alpha - \beta) = 1$ and $M^2 = 0$. The deviation increases rapidly for large m_Φ values due to the quartic power dependence of m_Φ, and it amounts to 50 (100)% for $m_\Phi = 300$ (400) GeV for $m_h = 120$ GeV. The larger deviation is obtained for the smaller value of m_h. The small "peak" structure in Fig. 2 originates from the threshold contribution when $m_\Phi = m_h$ for $\sqrt{q^2} = 2m_h$, where $\sqrt{q^2}$ is the invariant mass of the virtual h, i.e., the invariant mass of the two on-shell h Higgs bosons in the hhh vertex.

For nonzero values of M ($0 < M^2 < m_\Phi^2$), the magnitude of the loop correction is suppressed by the factor $(1 - M^2/m_\Phi^2)^3$, and the nondecoupling effect vanishes

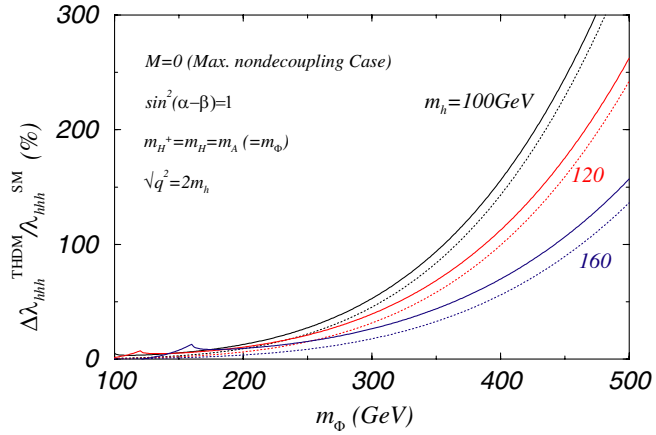

FIG. 2 (color online). $(\Delta \lambda_{hhh}^{\mathrm{THDM}}/\lambda_{hhh}^{\mathrm{SM}})$ is shown as a function of $m_\Phi (\equiv m_H = m_A = m_{H^{\pm}})$. The results of the full one-loop calculation are shown as solid curves, while the quartic mass (m_Φ^4) contributions, given in Eq. (95), are plotted as dotted curves.

VI. NUMERICAL EVALUATION

In this section, we present results of our numerical evaluation for the effective hZZ and hhh couplings predicted by the SM and the THDM at the one-loop order. We define the deviation from the SM prediction by

[3] Although the expression in Eq. (95) does not depend on $\tan\beta$, the allowed value of $\tan\beta$ is constrained to be $\mathcal{O}(1)$ due to the requirement of the perturbative unitarity when large values of m_Φ are taken with $M = 0$. Hence, the large deviation from the SM prediction occurs at $\tan\beta = \mathcal{O}(1)$. We note that the parameter set $m_H = m_A = m_{H^{\pm}}$, $M = 0$, $\alpha = \beta - \pi/2$ and $\tan\beta = 1$ corresponds to $\lambda_1 = \lambda_2 = \lambda_3 = (m_h^2 + m_H^2)/v^2$ and $\lambda_4 = \lambda_5 = -m_H^2/v^2$ at the tree level.

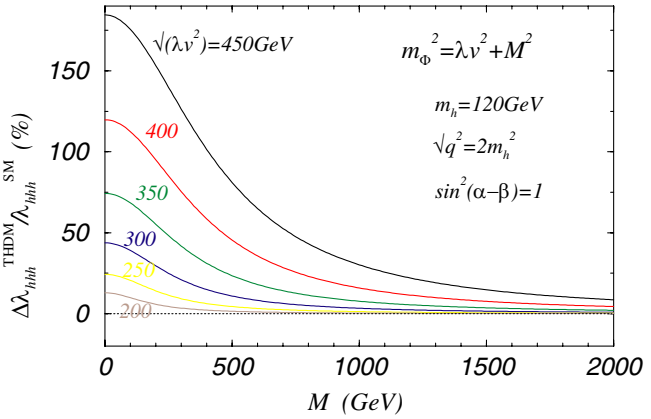

FIG. 3 (color online). The decoupling behavior of $(\Delta\lambda_{hhh}^{\rm THDM}/\lambda_{hhh}^{\rm SM})$ is shown. The mass of the heavy Higgs bosons $m_\Phi (\equiv m_H = m_A = m_{H^\pm})$ is given by $m_\Phi^2 = \lambda v^2 + M^2$.

when $M \simeq m_\Phi$. In Fig. 3, we show the decoupling behavior of the heavier Higgs contribution as a function of M with fixed $\sqrt{\lambda v^2} = 200$–450 GeV, in the case of $\sin^2(\alpha - \beta) = 1$ and $m_h = 120$ GeV, where the mass of the heavier Higgs bosons m_Φ $(= m_A = m_H = m_{H^\pm})$ is given by $m_\Phi^2 = \lambda v^2 + M^2$. (We note that λ corresponds to $\lambda_1 \cos^2\beta + \lambda_2 \sin^2\beta - m_h^2/v^2 = \lambda_3 - m_h^2/v^2 = -\lambda_4 = -\lambda_5$ in this case.) As shown, the heavier Higgs boson contributions reduce rapidly for a larger value of M. For $M = 1000$ GeV, the correction can be as large as a few tens of percent.

In Fig. 4, we show the momentum dependence of the deviation in the effective hhh coupling, $\Gamma_{hhh}(q^2)$ $(\equiv \Gamma_{hhh}(m_h^2, m_h^2, q^2))$, from the SM result as a function of the invariant mass $(\sqrt{q^2})$ of the virtual h boson, for various values of m_Φ $(= m_A = m_H = m_{H^\pm})$ with

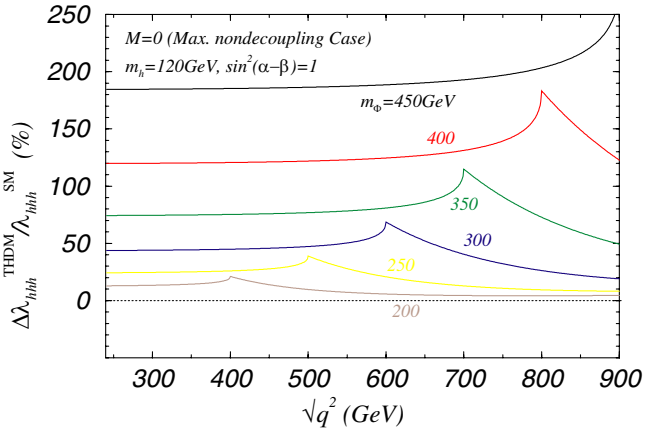

FIG. 4 (color online). The momentum dependence of $(\Delta\lambda_{hhh}^{\rm THDM}/\lambda_{hhh}^{\rm SM})$ is shown, where $\sqrt{q^2}$ is the invariant mass of h^* in $h^* \to hh$, for each value of m_Φ $(\equiv m_H = m_A = m_{H^\pm})$ when $m_h = 120$ GeV, $\sin(\alpha - \beta) = -1$, and $M = 0$.

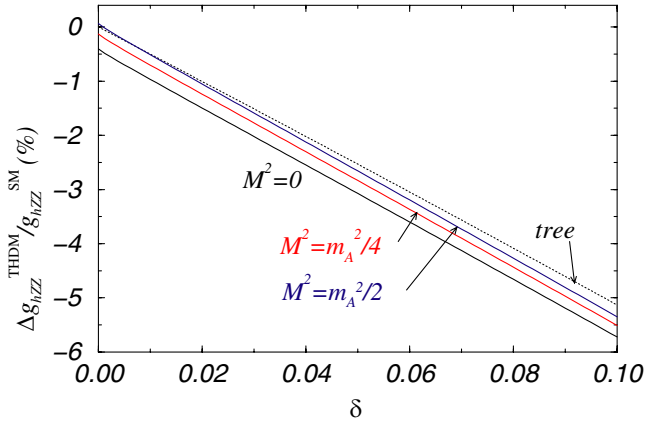

FIG. 5 (color online). Deviation of the one-loop renormalized (solid curves) and tree level (dotted curves) form factor M_1^{hZZ} from the SM value is shown as a function of $\delta = \cos^2(\alpha - \beta)$ for various M values. The other parameters are set to be $m_h = 120$ GeV, $\tan\beta = 2$, and $m_H = m_{H^\pm} = m_A = 300$ GeV.

$\sin^2(\alpha - \beta) = 1$ and $m_h = 120$ GeV. Again, to show the maximal nondecoupling effect, we have set M to be zero. The Higgs boson one-loop contribution is always positive. Below the peak of the threshold of the heavy Higgs pair production, $\Gamma_{hhh}(q^2)$ is insensitive to $\sqrt{q^2}$. We note that the low $\sqrt{q^2}$ (but $\sqrt{q^2} \gtrsim 2m_h$) is the most important region in the extraction of the hhh coupling from the data of the double Higgs production mechanism, because the h^* propagator $1/(q^2 - m_h^2)$ in the signal process becomes larger. On the contrary, as we have shown in Fig. 1 in Sec. II, the fermionic (top-quark) loop effect strongly depends on $\sqrt{q^2}$ because of the threshold enhancement at $\sqrt{q^2} = 2m_t$.

B. The mixing angle dependence

Here, we study the case in which the condition of $x = 0$ (or, $\sin(\alpha - \beta) = -1$) is relaxed. When $\sin(\alpha - \beta)$ is much different from -1, the renormalized couplings are significantly different from their SM values because of the tree level mixing effect [10,11]. Our main interest is rather the case in which the condition $\sin(\alpha - \beta) = -1$ is only slightly relaxed; i.e., $\sin(\alpha - \beta) \simeq -1$ or $x \ll 1$. We refer to such a case as the SM-like regime of the THDM. In order to study this case, we introduce the parameter $\delta = \cos^2(\alpha - \beta) = 1 - \sin^2(\alpha - \beta)$ $(\simeq x^2)$ which directly measures the deviation from the decoupling limit. In Figs. 5 and 6, we show $(\Delta g_{hZZ}^{\rm THDM}/g_{hZZ})$ and $(\Delta\lambda_{hhh}^{\rm THDM}/\lambda_{hhh})$ as a function of δ, respectively. The value of m_Φ $(= m_H = m_A = m_{H^\pm})$ is set to be 300 GeV. We consider the case of $m_h = 120$ GeV and $\tan\beta = 2$, and the scale M is taken to be 0, $m_A/2$, $m_A/\sqrt{2}$, and m_A. The solid curves are the results for the one-loop corrected couplings, and the dotted ones are for the tree level couplings.

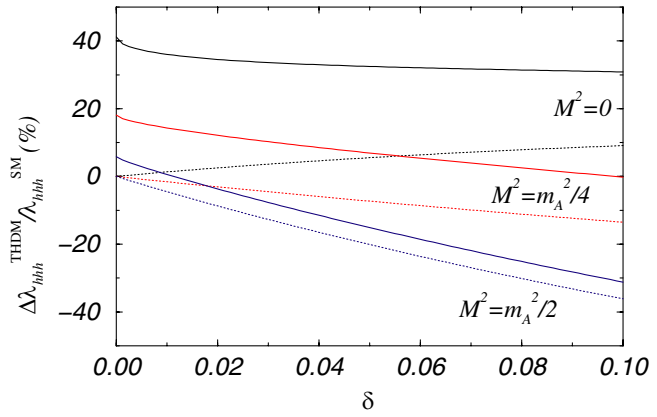

FIG. 6 (color online). Deviation of the one-loop renormalized (solid curves) and tree level (dotted curves) hhh form factor from the SM value is shown as a function of $\delta = \cos^2(\alpha - \beta)$ for various M values. The other parameters are set to be $m_h = 120$ GeV, $\tan\beta = 2$, and $m_H = m_{H^\pm} = m_A = 300$ GeV.

As shown in Fig. 5, the tree level mixing effect on the hZZ coupling is proportional to δ and the deviation from the SM value is negative. The nondecoupling effect on the hZZ coupling is insensitive to δ as long as δ is not large, and its deviation is less than 1% to the negative direction. The nondecoupling effect becomes maximal for $M = 0$, and minimum for $M = m_\Phi$.

Figure 6 shows that the deviation in the tree level hhh coupling can vary due to the Higgs mixing effect from -80 to $+10\%$ for $\delta = 0.1$, depending on the value of $0 < M^2/m_\Phi^2 < 1$. The deviation of the tree level hhh coupling vanishes as $\delta = 0$, which reproduces the SM case. For the fixed value of δ, smaller M^2 gives larger value (in magnitude) of the tree level hhh coupling. At one-loop level, the nondecoupling effect of the heavy Higgs bosons gives large positive corrections to $(\Delta\lambda_{hhh}^{\rm THDM}/\lambda_{hhh}^{\rm SM})$. Because of the nondecoupling effect, the deviation in the one-loop hhh coupling can be plus 40% for $M = 0$, even when $\delta = 0$. Though the deviation decreases when δ increases, such large positive contribution remains for $\delta = 0.1$. For $M = m_\Phi/2$ the magnitude of the nondecoupling effect is smaller than that for $M = 0$. However, the deviation can still be larger than that induced at tree level by the Higgs mixing effect for $0 < M^2/m_\Phi^2 < 1$, especially in the region of $0 < \delta < 0.06$.

In conclusion, the large nondecoupling effect of the heavier Higgs bosons contributing in loops can be more important than the tree level Higgs mixing effect, as long as δ is not too large.

C. The possible allowed region of the corrections

Finally, we study possible allowed range of the deviation in the hZZ and hhh couplings from the SM predictions under the experimental and theoretical constraints. The free parameters of the Higgs sector in the THDM (m_h, m_H, m_A, $m_{H^\pm}$, α, β, and M) are constrained by theoretical consideration as well as the available experimental data. These are related to the quartic coupling constants in Eq. (7) by Eqs. (23) to (27). We take into account the following bounds in order to constrain the parameters.

(i) The coupling constants λ_i $(i = 1 - 5)$ are constrained by the requirement of perturbative unitarity [35], which is described by the condition on the S-wave amplitudes for the elastic scattering of longitudinally polarized gauge bosons as well as the Higgs bosons [34];

$$|a^0(\varphi_A\varphi_B \to \varphi_C\varphi_D)| < \xi, \tag{98}$$

where $a^0(\varphi_A\varphi_B \to \varphi_C\varphi_D)$ is the S-wave amplitude for the elastic scattering process $\varphi_A\varphi_B \to \varphi_C\varphi_D$ of the longitudinally polarized gauge bosons (and Higgs bosons); cf. Appendix D. The critical value ξ is a parameter, and we here take $\xi = 1/2$ in our analysis [21].

(ii) The condition of vacuum stability is expressed at the tree level by [37]

$$\lambda_1 > 0, \qquad \lambda_2 > 0,$$
$$\sqrt{\lambda_1\lambda_2} + \lambda_3 + \mathrm{MIN}(0, \lambda_4 + \lambda_5, \lambda_4 - \lambda_5) > 0. \tag{99}$$

(iii) The LEP precision data imposed strong constraints on the radiative corrections to the gauge boson two-point functions, which are parametrized by the S, T, and U parameters [41]. In the THDM, the T parameter [$\simeq \alpha_{EM}^{-1}\Delta\rho$, where $\Delta\rho(\sim 10^{-3})$ is the deviation of ρ parameter from unity] can receive large contributions. The analytic formula for $\Delta\rho$ in the THDM is given, for example, in Refs. [38,39]. To satisfy this constraint, the THDM has to have an approximate custodial [$SU(2)_V$] symmetry [43]. In the Higgs sector of the THDM, there are typically two options for the parameter choice in which $SU(2)_V$ is conserved according to the assignment of the $SU(2)_V$ charge; (1) $m_{H^\pm} \simeq m_A$, and (2) $m_{H^\pm} \simeq m_H$ with $\sin^2(\alpha - \beta) \simeq 1$ or $m_{H^\pm} \simeq m_h$ with $\cos^2(\alpha - \beta) \simeq 1$ [38,43][4].

In the present paper, we do not perform a complete scan analysis for all the parameter space. Instead, we set $m_H = m_A = m_{H^\pm}$ in order to reduce the number of parameters. By the degeneracy of heavy Higgs bosons, the constraint from the ρ parameters is satisfied. Then, the free parameters are m_A, $\tan\beta$, M, as well as δ (or α).

[4]In terms of the coupling constants, these conditions are expressed by (1) $\lambda_4 = \lambda_5$, and (2) $\lambda_1 = \lambda_2 = \lambda_3$ with $m_1^2 = m_2^2$.

In Figs. 7 and 8, we show the allowed region of $(\Delta g_{hZZ}^{\rm THDM}/g_{hZZ}^{\rm SM})$ and $(\Delta\lambda_{hhh}^{\rm THDM}/\lambda_{hhh}^{\rm SM})$ for $M = 0$ as a function of δ $(0 < \delta < 0.5)$, respectively. The mass of the lightest Higgs boson is set to be $m_h = 120$ GeV. In Fig. 7, we find that the nondecoupling loop effect on the hZZ coupling is at most a few percent. Because of the leading contribution of the additional Higgs bosons, the correction becomes negative. Most of the deviation from the SM prediction comes from the tree level mixing effect of the factor $\sin^2(\alpha - \beta)$. On the other hand, as shown in Fig. 8, due to the nondecoupling effect of the heavy Higgs bosons the allowed region of $\Delta\lambda_{hhh}^{\rm THDM}/\lambda_{hhh}^{\rm SM}$ becomes much wider than that for the tree level. The correction can be as large as a few hundred percent. We note that such large deviation from the SM prediction cannot be realized solely by the tree level Higgs mixing effect for $0 < \delta < 0.5$.

As the typical case for the nonzero value of M, we show the result for $M = m_\Phi/2$ in Figs. 9 and 10, where $m_\Phi \equiv m_H = m_A = m_{H^\pm}$. All the other parameters are taken to be the same as those in Figs. 7 and 8. As shown, the magnitude of the nondecoupling effect becomes smaller as compared to the case with $M = 0$, both in the hZZ and hhh couplings, because of the suppression factor $(1 - M^2/m_\Phi^2)^n$; cf. Eqs. (94) and (95). In the hhh coupling, the tree level mixing effect becomes significant for larger values of δ, by which the positive contribution due to the nondecoupling effect is canceled: cf. Eq. (95). The deviation from the SM prediction can be larger than a few hundred percent for the small values of δ.

Some comments are in order related to the unitarity constraint. If we take $\xi = 1$ [34] instead of $\xi = 1/2$ [21], the constraint from the perturbative unitarity is relaxed on both the tree level and loop effects. Then larger values of m_Φ can be taken, so that the possible enhancement due to the nondecoupling loop effect becomes greater. The rate of enhancement due to the change from $\xi = 1/2$ to $\xi = 1$ is much larger at one-loop level than that at tree level.

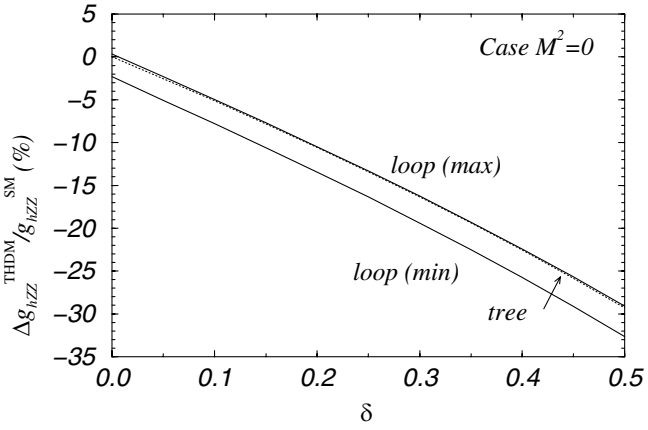

FIG. 7. Allowed region of the deviation in the form factor M_1^{hZZ} under the constraints obtained from perturbative unitarity and vacuum stability as a function of $\delta[= \cos^2(\alpha - \beta)]$. We set $m_H = m_A = m_{H^\pm}$, and the value of M is fixed to be zero in order to study the maximal nondecoupling effect. The upper and lower limits for the one-loop renormalized couplings are shown as solid curves. The value of the tree level one is shown as the dotted curve.

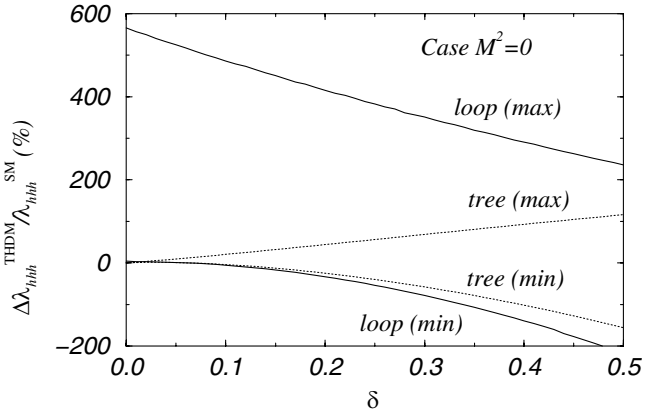

FIG. 8. Allowed region of the deviation in the hhh form factor under the constraints obtained from perturbative unitarity and vacuum stability as a function of $\delta[= \cos^2(\alpha - \beta)]$. We set $m_H = m_A = m_{H^\pm}$, and the value of M is fixed to be zero in order to study the maximal nondecoupling effect. The upper and lower limits for the one-loop renormalized couplings are shown as solid curves. Those for the tree level couplings are shown as dotted curves.

D. Discussions

Before concluding this section, we give a few comments on our analysis.

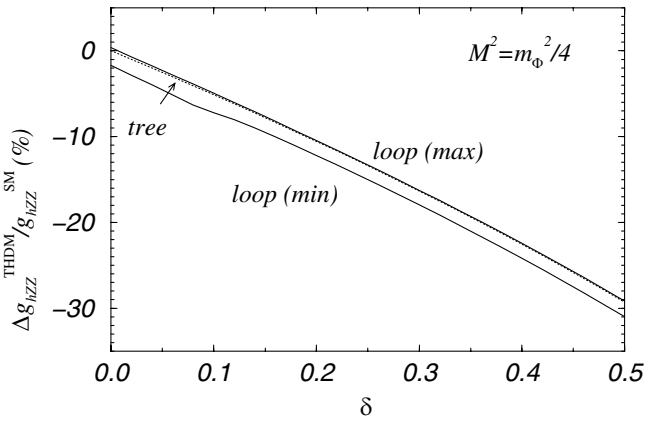

FIG. 9. Allowed region of the deviation in the form factor M_1^{hZZ} under the constraints obtained from perturbative unitarity and vacuum stability as a function of $\delta[= \cos^2(\alpha - \beta)]$. We set $m_H = m_A = m_{H^\pm}(\equiv m_\Phi)$, and the value of M is fixed to be $m_\Phi/2$. The upper and lower limits for the one-loop renormalized couplings are shown as solid curves. The value of the tree level one is shown as the dotted curve.

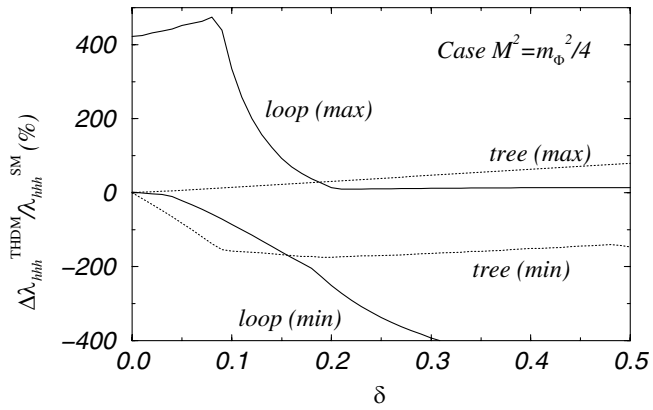

FIG. 10. Allowed region of the deviation in the hhh form factor under the constraints obtained from perturbative unitarity and vacuum stability as a function of $\delta[=\cos^2(\alpha-\beta)]$. We set $m_H = m_A = m_{H^\pm}(\equiv m_\Phi)$, and the value of M is fixed to be $m_\Phi/2$. The upper and lower limits for the one-loop renormalized couplings are shown as solid curves. Those for the tree level couplings are shown as dotted curves.

The large one-loop radiative correction of $\mathcal{O}(1)$ to the coupling λ_{hhh} in the THDM does not imply the breakdown of the perturbative expansion, because the large contribution originates from new types of couplings, e.g., $\lambda_{h\Phi\Phi}$ and $\lambda_{hh\Phi\Phi}$, that enter in loop calculations. Needless to say, we do not expect such kind of large correction to occur beyond the one-loop order.

We have shown the results by assuming Model II for the Yukawa interaction. In the case of Model I, our main results presented thus far are essentially unchanged when h approximately behaves like the SM Higgs boson. It is well-known that in Model II, the $b \to s\gamma$ data imposed a strong constraint on the mass of the charged Higgs boson. We have not explicitly included the constraint from the $b \to s\gamma$ data [44] in our analysis, which can be easily satisfied by assuming that the mass of the charged Higgs boson is larger than about 300 GeV. In Model I, there is no such strong constraint from the $b \to s\gamma$ data.

The measurement of the hZZ and hhh couplings are important not only to confirm the mechanism of the electroweak symmetry breaking, but also to indirectly explore the property of new physics beyond the SM. In particular, when the lightest Higgs boson h is found to be around 120 GeV at the LHC or LCs, and if its coupling with the gauge boson (hZZ or hWW) is SM-like, the measurement of the hhh coupling becomes important to determine the scale of the new physics. If the measured hhh coupling turns out to be much larger than the SM prediction and is not possible to be explained by the tree level mixing effect in the THDM, we may consider the strongly-coupled THDM with a relatively low cutoff scale. Such large deviation in the hhh coupling could be the first indirect signal for the models of dynamical symmetry breaking [22], or models of electroweak baryogenesis [23,45]. Otherwise, the model with a light h should indicate a weakly-coupled theory [46].

The trilinear coupling of the lightest Higgs boson can be measured from studying the scattering processes $e^+e^- \to Z^* \to Zh^* \to Zhh$ and $e^+e^- \to \bar{\nu}\nu W^{+*}W^{-*} \to \bar{\nu}\nu h^* \to \bar{\nu}\nu hh$ in the e^+e^- collision, and $\gamma\gamma \to h^* \to hh$ at the $\gamma\gamma$ option of the LC. In Fig. 4, the momentum dependence on the self-coupling has been shown in the SM-like limit. The corrections turned out to be insensitive for the energy below the threshold of the pair production of the loop particles [14]. Therefore, our main conclusion for the form factors of the hhh coupling shown in this paper can be applied to the momentum dependent coupling included in the above production processes as a good approximation. However, the large positive deviation in the hhh coupling does not necessarily imply the large deviation in the production cross sections by the same rate, because the rest of the gauge invariant set of Feynman diagrams usually do not contain the hhh vertex. There have been several studies for the correlation between the change of the hhh coupling and the production cross sections at the LHC [9] and LCs [7,8,20]. From the conclusions in those studies, we expect that the large nondecoupling effect in the hhh couplings in the THDM can be detected at future experiments at the LCs.

We finally comment on the case of the MSSM. Since the Higgs sector of the MSSM is a special case of the Model II THDM with $\lambda_i v^2 \simeq \mathcal{O}(m_W^2)$, as required by supersymmetry, it belongs to the class of models in which the heavier Higgs bosons decouple. Hence, the effect of the Higgs boson loops to $\Gamma_{hhh}(MSSM)$ is expected to be small. A detailed study on this decoupling behavior of the one-loop corrected hhh coupling in the MSSM can be found in Refs. [12,13]. We confirmed that our results for large values of M are consistent with those in Ref. [12].

VII. CONCLUSION

We have discussed the one-loop contributions of the heavy additional Higgs bosons to the hZZ and hhh couplings in the THDM. The form factors have been calculated in the on-shell scheme, and the deviation from the SM predictions are evaluated.

The renormalized couplings of hZZ and hhh can deviate from the SM predictions due to two origins: the tree level mixing effect between the Higgs bosons and the quantum effect of the additional particles in the loop. We found that the deviations in the form factors can be large due to the nondecoupling effect of the heavy additional Higgs bosons when their masses are predomi-

nantly generated from the vacuum expectation value of the electroweak symmetry breaking; i.e., in a strongly-coupled THDM. In particular, the renormalized hhh coupling can largely deviate from the SM prediction due to the quartic power term of the masses of the heavy Higgs bosons, especially when the mass of the lightest Higgs boson h is relatively small. Even in the case where approximately only h couples to the weak gauge boson so that the mixing effect is small, the deviation in the hhh coupling from the SM value can be as large as a few hundred percent, while that in the hZZ coupling is at most a few times of -1% or less. When the tree level mixing effect of the Higgs bosons is significant, the deviation in the hZZ coupling becomes significant by the factor of $\sin(\beta-\alpha)$, while the large positive deviation in the hhh coupling due to quantum effect is smeared by the mixing effect. Such large quantum effect on the Higgs trilinear coupling is distinguishable from the Born-level mixing effect, and can be detectable at a linear collider.

In the weakly-coupled THDM, where the masses of the heavy Higgs bosons are predominantly generated from the soft-breaking mass term M, the one-loop effect is small and decouples in the large mass limit.

We have shown how the nondecoupling effect of the additional heavy particles in the THDM can differ the Higgs boson couplings hZZ and hhh from the SM prediction. We stress that the quartic mass effect on the effective hhh coupling is a general characteristic in any new physics model which has the nondecoupling property.

ACKNOWLEDGMENTS

We thank Shingo Kiyoura for useful discussions and Ilya Ginzburg for indicating a typo in the text. S. K. and C. P. Y. thank the hospitality of the National Center for Theoretical Sciences in Taiwan, ROC, where part of this work was completed. The work of Y. O. was supported in part by Grants-in-Aid of the Ministry of Education, Culture, Sports, Science, and Technology, Government of Japan, Grant Nos. 13640309 and 13135225. The work of C. P. Y. was supported in part by NSF Grant No. PHY-0244919.

APPENDIX A: IN THE STANDARD MODEL

Here, we show the calculation for the one-loop contributions of the top quark to the form factors of hZZ and hhh vertices in the SM. The formulas for the leading top-loop contributions in Eqs. (5) and (6) are extracted from the results shown in Appendix A 1. The appearance of the quartic mass dependence of the top quark in the hhh coupling in Eq. (6) can also be shown through the effective potential method in Appendix A 2. Here, we consider only the third generation quarks (the top and bottom quarks) as the matter fields.

1. Diagrammatic method

The Lagrangian of the SM is given by

$$\begin{aligned}\mathcal{L}_{\rm SM} = &+\overline{Q}_L D_\mu \gamma^\mu Q_L + \bar{t}_R D_\mu \gamma^\mu t_R + \overline{b}_R D_\mu \gamma^\mu b_R \\ &- \{y_b \overline{Q}_L \Phi b_R + y_t \tilde{\Phi} Q_L t_R + \text{h.c.}\} + |D^\mu \Phi|^2 \\ &- V_{\rm SM},\end{aligned} \tag{A1}$$

where $Q_L = (t_L, b_L)^T$, and D_μ is the covariant derivative. The Higgs potential is defined by

$$V_{\rm SM} = -\mu^2|\Phi|^2 + \lambda|\Phi|^4, \tag{A2}$$

with the isodoublet field Φ being parametrized as

$$\Phi = \begin{bmatrix} w^+ \\ \frac{1}{\sqrt{2}}(v + h + iz) \end{bmatrix}, \tag{A3}$$

where v ($\simeq 246$ GeV) is the vacuum expectation value, h is the Higgs boson, and $w^\pm$ and z are the would-be Nambu-Goldstone bosons.

The kinematic term for the Higgs doublet field Φ yields

$$\mathcal{L}_{hZZ} = \frac{m_Z^2}{v} g_{\mu\nu} Z^\mu Z^\nu h, \tag{A4}$$

where we used the relation $m_Z^2 = \frac{g^2+g'^2}{4} v^2$. The tree level form factors of hZZ vertices are given by

$$M_1^{hZZ} = \frac{2m_Z^2}{v}, \qquad M_2^{hZZ} = M_3^{hZZ} = 0. \tag{A5}$$

From the Higgs potential (A2), we have

$$V_{\rm SM} = -T_h h + \frac{1}{2}(m_h^2 - \frac{T_h}{v})h^2 + \frac{m_h^2}{2v} h^3 + \frac{m_h^2}{8v^2} h^4 + \cdots, \tag{A6}$$

where we introduced the parameters T_h and m_h^2 by

$$T_h = v(\mu^2 - \lambda v^2), \qquad m_h^2 = 2\lambda v^2, \tag{A7}$$

and eliminated μ and λ. The vacuum condition (the stationary condition) requires that the one-point function vanishes at the vacuum. At the tree level, this implies that $T_h = 0$, so that the parameter m_h denotes the mass of h. The Higgs self-coupling interaction is expressed at tree level by

$$\Gamma_{hhh}^{\rm tree} = -\frac{3m_h^2}{v}, \qquad \Gamma_{hhhh}^{\rm tree} = -\frac{3m_h^2}{v^2}. \tag{A8}$$

The Yukawa interaction generates the mass of the quarks, and $m_t = y_t \frac{v}{\sqrt{2}}$. Furthermore, the parameters of the Lagrangian g, g', v, λ, μ, and y_t can be replaced by m_Z, m_W, v, T_h, m_h^2, and m_t.

The bare parameters of the model can be rewritten in terms of the renormalized parameters as

$$m_V^2 \to m_V^2 + \delta m_V^2, \qquad (V = W, Z) \tag{A9}$$

$$v \to v + \delta v, \tag{A10}$$

$$T_h \to T_h + \delta T_h, \tag{A11}$$

$$m_h^2 \to m_h^2 + \delta m_h^2, \tag{A12}$$

and the wave function renormalization factors are introduced with the renormalized fields by

$$Z^\mu \to Z_Z^{1/2} Z^\mu + C_{Z\gamma} A^\mu = \left(1 + \frac{1}{2}\delta Z_Z + \cdots\right) Z^\mu + (\delta Z_{Z\gamma} + \cdots) A^\mu, \tag{A13}$$

$$h \to Z_h^{1/2} h = \left(1 + \frac{1}{2}\delta Z_h + \cdots\right) h. \tag{A14}$$

From the kinematic term, we obtain the counterterm for the hZZ interaction,

$$\mathcal{L}_{hZZ} \to \frac{m_Z^2}{v}\left(1 + \frac{\delta m_Z^2}{m_Z^2} - \frac{\delta v}{v}\right) g_{\mu\nu} Z^\mu Z^\nu h \left(1 + \delta Z_Z + \frac{1}{2}\delta Z_h + \cdots\right) \to \frac{m_Z^2}{v} g_{\mu\nu} Z^\mu Z^\nu h \left(1 + \frac{\delta m_Z^2}{m_Z^2} - \frac{\delta v}{v} + \delta Z_Z + \frac{1}{2}\delta Z_h\right). \tag{A15}$$

We here neglect the effect of the Z-γ mixing, because it is of $\mathcal{O}(\alpha_{\rm EM})$. Thus, we have the counterterm for the hZZ form factors as

$$\delta M_1^{hZZ} = \frac{2m_Z^2}{v}\left(\frac{\delta m_Z^2}{m_Z^2} - \frac{\delta v}{v} + \delta Z_Z + \frac{1}{2}\delta Z_h\right), \qquad \delta M_2^{hZZ} = \delta M_3^{hZZ} = 0. \tag{A16}$$

The bare Higgs Lagrangian can be rewritten as

$$\begin{aligned}\mathcal{L}_{\rm Higgs} \to{}& +\frac{1}{2}p^2(1+\delta Z_h)h^2 + \left\{(\mu^2 - \lambda v^2)\left(1 + \frac{1}{2}\delta Z_h\right) + (\delta\mu^2 - \delta\lambda v^2 - 2\lambda v\delta v)\right\}(v + \delta v)h - \frac{1}{2}\{(\mu^2 - 3\lambda v^2) \\ &\times (1 + \delta Z_h) + (\delta\mu^2 - 3\delta\lambda v^2 - 6\lambda v\delta v)\}h^2 - \left(\lambda v + \delta\lambda v + \lambda\delta v + \frac{3}{2}\lambda v\delta Z_h\right)h^3 - \frac{1}{4}(\lambda + \delta\lambda + 2\lambda\delta Z_h)h^4 \\ ={}& \mathcal{L}_{\rm Higgs} + \delta T_h h + \frac{1}{2}\left\{(p^2 - m_h^2)\delta Z_h - \delta m_h^2 + \frac{\delta T_h}{v}\right\}h^2 - \left\{\frac{\delta m_h^2}{2v} + \frac{m_h^2}{2v}\left(-\frac{\delta v}{v} + \frac{3}{2}\delta Z_h\right)\right\}h^3 \\ &- \frac{1}{4}\left\{\frac{\delta m_h^2}{2v^2} + \frac{m_h^2}{v^2}\left(-\frac{\delta v}{v} + \delta Z_h\right)\right\}h^4,\end{aligned} \tag{A17}$$

where δT_h and δm_h^2 are consistently related to the shift of the Lagrangian parameters μ and λ by

$$\delta T_h \equiv (\delta\mu^2 - \delta\lambda v^2 - 2\lambda v\delta v)v = \delta\{v(\mu^2 - \lambda v^2)\}, \tag{A18}$$

$$\delta m_h^2 \equiv 2\delta\lambda v^2 + 4\lambda v\delta v = \delta(2\lambda v^2). \tag{A19}$$

The counterterm for the hhh and $hhhh$ vertices are

$$\delta\Gamma_{hhh} = -\left\{\frac{3\delta m_h^2}{v} + \frac{3m_h^2}{v}\left(-\frac{\delta v}{v} + \frac{3}{2}\delta Z_h\right)\right\}, \tag{A20}$$

$$\delta\Gamma_{hhhh} = -\left\{\frac{3\delta m_h^2}{v^2} + \frac{6m_h^2}{v^2}\left(-\frac{\delta v}{v} + \delta Z_h\right)\right\}. \tag{A21}$$

Based on Eqs. (A16) and (A20), we have to provide the counterterm parameters δm_h^2, δZ_h, δv, δm_Z^2, δZ_Z in order to calculate the one-loop form factors of hZZ and hhh. In the following, we determine all these parameters by imposing proper renormalization conditions.

The renormalization is performed in the on-shell scheme [27]. The counterterms of the gauge boson masses (δm_W^2, δm_Z^2) and wave functions (δZ_W, δZ_Z) are obtained by calculating the transverse part $\Pi_T^{VV}(p^2)$ of the two-point function

$$\Pi_{\mu\nu}^{VV}(p^2) = \left(-g_{\mu\nu} + \frac{p_\mu p_\nu}{p^2}\right)\Pi_T^{VV}(p^2) + \frac{p_\mu p_\nu}{p^2}\Pi_L^{VV}(p^2), \tag{A22}$$

where $VV = WW$ or ZZ. In the on-shell renormalization scheme, we obtain

$$\delta m_Z^2 = {\rm Re}\Pi_T^{ZZ(1{\rm PI})}(m_Z^2), \tag{A23}$$

$$\delta Z_Z = -\frac{\partial}{\partial p^2}{\rm Re}\Pi_T^{ZZ(1{\rm PI})}(p^2)\Big|_{p^2 = m_Z^2}. \tag{A24}$$

We define δv by

$$\frac{\delta v}{v} = \frac{1}{2}\frac{1}{m_W^2}\mathrm{Re}\Pi_T^{WW(1\mathrm{PI})}(0) + (\text{vertex and box corrections}), \quad \text{(A25)}$$

where the "(vertex and box corrections)" in Eq. (A25) is $\mathcal{O}(\alpha_{EM})$, and is neglected in our calculations.

The other counterterms δT_h, δm_h^2, and δZ_h are determined in the following way. First, the tadpole must be zero after renormalization; i.e., at tree level we demand $T_h = v(\mu^2 - \lambda v^2) = 0$, and at one-loop level, we impose

$$\Gamma_h^R \equiv T_h^{\mathrm{tree}} + T_h^{1\mathrm{PI}} + \delta T_h = 0, \quad \text{(A26)}$$

where Γ_h^R is the renormalized tadpole and $T_h^{1\mathrm{PI}}$ is the one-loop Feynman diagram of the tadpole (cf. Appendix A 3). This determines the counterterm δT_h as

$$\delta T_h = -T_h^{1\mathrm{PI}}. \quad \text{(A27)}$$

Second, we determine the rest of the counterterms in the on-mass shell scheme, i.e.,

$$\mathrm{Re}\Gamma_{hh}^R[m_h^2] = 0, \quad \text{(A28)}$$

$$\frac{\partial}{\partial p^2}\mathrm{Re}\Gamma_{hh}^R[p^2]\Big|_{p^2=m_h^2} = 1, \quad \text{(A29)}$$

where $\Gamma_{hh}^R[p^2]$ is the renormalized two-point function of hh:

$$\Gamma_{hh}^R[p^2] = (p^2 - m_h^2)(1 + \delta Z_h) - \delta m_h^2 + \frac{\delta T_h}{v} + \Pi_{hh}^{1\mathrm{PI}}(p^2), \quad \text{(A30)}$$

and $\Pi_{hh}^{1\mathrm{PI}}(p^2)$ is the 1PI Feynman diagram contribution (cf. Appendix A 3). Therefore, we obtain

$$\delta m_h^2 = +\mathrm{Re}\Pi_{hh}^{1\mathrm{PI}}(m_h^2) - \frac{1}{v}\mathrm{Re}T_h^{1\mathrm{PI}}, \quad \text{(A31)}$$

$$\delta Z_h = -\frac{\partial}{\partial p^2}\mathrm{Re}\Pi_{hh}^{1\mathrm{PI}}(p^2)\Big|_{p^2=m_h^2}. \quad \text{(A32)}$$

Using the counterterms δm_Z, δZ_Z, δv, δT_h, δm_h^2, and δZ_h which are determined above with the 1PI diagrams listed in Appendix A 3, we obtain the renormalized form factors of hZZ and hhh. Consequently, the renormalized form factors are given by

$$M_i^{hZZ}(p_1^2, p_2^2, q^2) = M_i^{hZZ(\mathrm{tree})} + M_i^{hZZ(1\mathrm{PI})} + \delta M_i^{hZZ}, \quad (i = 1 - 3), \quad \text{(A33)}$$

$$\Gamma_{hhh}(p_1^2, p_2^2, q^2) = \Gamma_{hhh}^{\mathrm{tree}} + \Gamma_{hhh}^{1\mathrm{PI}} + \delta\Gamma_{hhh}, \quad \text{(A34)}$$

where the momentum q^μ in Eq. (A33) is that of the external Higgs boson line. The leading contributions of the top-quark mass in Eqs. (5) and (6) can be obtained from Eqs. (A33) and (A34) by taking the large m_t limit in the explicit expressions of each diagram contribution listed in A 3

2. Effective potential method

The quartic power dependence of the top-quark mass can be reproduced in the effective potential method. The effective potential provides the information of vertex functions with zero external momenta at each loop level. The one-loop effective potential is given by

$$V_{\mathrm{eff}}[\varphi] = V_{\mathrm{tree}}[\varphi] + \frac{1}{64\pi^2}N_{c_f}N_{s_f}(-1)^{2s_f}M_f^4[\varphi] \times \left(\ln\left[\frac{M_f^2}{Q^2}\right] - \frac{3}{2}\right), \quad \text{(A35)}$$

where $\varphi = \langle\phi\rangle = v + \langle h\rangle$, N_{c_f} is the color number, s_f (N_{s_f}) is the spin (degree of freedom) of the field f in the loop, $M_f[\varphi]$ is the field dependent mass of f, and Q is an arbitrary scale.

The bare parameters μ^2 and λ in the SM Higgs potential $V_{\mathrm{SM}}[\varphi]$ in Eq. (A2) ($= V_{\mathrm{tree}}[\varphi]$) can be eliminated after introducing the one-loop corrected vacuum expectation value v and the mass m_h in the following conditions:

$$\frac{\partial}{\partial\varphi}V_{\mathrm{eff}}[\varphi]\Big|_{\varphi=v} = 0, \quad \text{(A36)}$$

$$\frac{\partial^2}{\partial\varphi^2}V_{\mathrm{eff}}[\varphi]\Big|_{\varphi=v} = m_h^2. \quad \text{(A37)}$$

Let us consider the top-quark loop effect. Namely, in Eq. (A35), $f = t$, $N_{C_t} = 3$, $N_{S_t} = 2$, and the field dependent mass of t is given by

$$M_t[\varphi] = y_t\frac{\varphi}{\sqrt{2}}. \quad \text{(A38)}$$

The result (6) of the renormalized coupling constant $\Gamma_{hhh}^{\mathrm{SM}}$ is then obtained from

$$\frac{\partial^3}{\partial\varphi^3}V_{\mathrm{eff}}[\varphi]\Big|_{\varphi=v} = 3\frac{m_h^2}{v}\left\{1 - \frac{N_{c_t}}{3\pi^2}\frac{m_t^4}{v^2 m_h^2}\right\}, \quad \text{(A39)}$$

where m_t is the mass of the top quark. Because the top quark is a fermion, its loop effect on the effective potential is negative.

Let us examine the origin of this quartic mass contribution. If we write $\varphi = v_0 + h$, then the effective potential is

$$V_{\rm eff} = -\frac{\mu^2}{2}(v_0+h)^2 + \frac{1}{4}\lambda(v_0+h)^4 - \frac{N_c}{16\pi^2}\frac{y_t^4}{4}(v_0+h)^4\left[\ln\frac{y_t^2 v_0^2(1+\frac{h}{v_0})^2}{2Q^2} - \frac{3}{2}\right] = -\frac{\mu^2}{2}(v_0+h)^2 + \frac{1}{4}\tilde{\lambda}(v_0+h)^4 - \frac{N_c}{16\pi^2}\frac{y_t^4}{2}v_0^4\left(\frac{h}{v_0}+\frac{7}{2}\frac{h^2}{v_0^2}+\frac{13}{3}\frac{h^3}{v_0^3}+\cdots\right), \quad \text{(A40)}$$

where

$$\tilde{\lambda} \equiv \lambda - \frac{N_c}{16\pi^2}y_t^4\left(\ln\frac{y_t^2 v_0^2}{2Q^2} - \frac{3}{2}\right). \quad \text{(A41)}$$

The first to third derivatives are calculated as

$$\frac{\partial V_{\rm eff}}{\partial h} = -\mu^2 v_0 + \tilde{\lambda}v_0^3 - \frac{1}{2}\frac{N_c}{16\pi^2}y_t^4 v_0^3, \quad \text{(A42)}$$

$$\frac{\partial^2 V_{\rm eff}}{\partial h^2} = -\mu^2 + 3\tilde{\lambda}v_0^2 - \frac{7}{2}\frac{N_c}{16\pi^2}y_t^4 v_0^2, \quad \text{(A43)}$$

$$\frac{\partial^3 V_{\rm eff}}{\partial h^3} = 6\tilde{\lambda}v_0 - 13\frac{N_c}{16\pi^2}y_t^4 v_0. \quad \text{(A44)}$$

Using Eqs. (A36) and (A37), we can eliminate μ^2 and $\tilde{\lambda}$ by introducing the renormalized (at zero momentum) mass m_h^2. Then, we obtain the renormalized coupling $\lambda_{hhh}^{\rm SM}$, as given in Eq. (A39). The logarithmic term in the effective potential is completely eliminated by the mass renormalization. On the contrary, the higher dimensional operator terms in the effective potential generally survive even after the mass renormalization, which yield the $\mathcal{O}(m_t^4)$ correction to the tree level hhh coupling.

3. 1PI diagram contributions in the SM

We list the relevant one-particle irreducible (1PI) n-point functions for $n = 1, 2, 3$. The calculation is performed in Landau gauge, so that the Nambu-Goldstone bosons are massless ($m_{w^\pm} = m_z = 0$). The SM Higgs boson coupling constants to be used below are defined as

$$\lambda_{hhh}v = \lambda_{hzz}v = \frac{1}{2}\lambda_{hw^+w^-}v = 4\lambda_{hhhh}v^2 = 2\lambda_{hhzz}v^2 = \lambda_{hhw^+w^-}v^2 = -\frac{m_h^2}{2}.$$

A. One- and two-point functions

The one-loop top-bottom contributions and the Higgs scalar contributions to $\Pi_T^{ZZ}(p^2)$ and $\Pi_T^{WW}(p^2)$ are given by

$$\Pi_T^{ZZ}(p^2) = -\frac{N_c}{16\pi^2}\frac{16m_Z^2}{v^2}\Big[\Big(\frac{1}{2}I_f^2 - I_f Q_f s_W^2 + Q_f^2 s_W^4\Big)\times\{(D-2)B_{22} + p^2(B_1+B_{21})\} + (I_f - Q_f s_W^2)Q_f s_W^2 m_f^2 B_0\Big](p^2, m_f, m_f) + \frac{1}{16\pi^2}\frac{m_Z^2}{v^2}\{c_{2W}^2 B_5(p^2; m_{w^\pm}, m_{w^\pm}) + B_5(p^2, m_z, m_h)\} \quad \text{(A45)}$$

$$\Pi_T^{WW}(p^2) = -\frac{N_c}{16\pi^2}\frac{m_W^2}{v^2}\{(D-2)4B_{22} + 4p^2(B_1+B_{21})\}\times(p^2; m_t, m_b) + \frac{1}{16\pi^2}\frac{m_W^2}{v^2}\{B_5(p^2; m_{w^\pm}, m_z) + B_5(p^2; m_w, m_h)\}, \quad \text{(A46)}$$

where we used the Passarino-Veltman functions [47] for the tensor coefficients of the loop integrals, and we define $B_5(p^2; m_1, m_2) = A(m_1) + A(m_2) - 4B_{22}(p^2; m_1, m_2)$. I_f and Q_f are the isospin quantum number and the electric charge of the fermion f, respectively. For example, $I_f = 1/2$ and $Q_f = 2/3$ for $f = t$. Also, $s_W = \sin\theta_W$, where θ_W is the weak-mixing angle. The 1PI tadpole contributions are calculated as

$$T_h^{\rm 1PI} = \sum_{f=t,b}\Big\{-\frac{N_c}{16\pi^2}\frac{4m_f^2}{v}A(m_f)\Big\} - \frac{1}{16\pi^2}3\lambda_{hhh}A(m_h). \quad \text{(A47)}$$

The 1PI diagram contributions to the Higgs boson two-point function is obtained as

$$\Pi_{hh}^{\rm 1PI}(p^2) = \sum_{f=t,b}\Big[-\frac{N_c}{16\pi^2}\frac{m_f^2}{v^2}\{4A(m_f) + (-2p^2+8m_f^2)B_0(p^2; m_f, m_f)\}\Big] + \frac{1}{16\pi^2}\{+(\lambda_{hww})^2 B_0(p^2; m_w, m_w) + 2(\lambda_{hzz})^2 B_0(p^2; m_z, m_z) + 18(\lambda_{hhh})^2 B_0(p^2; m_h, m_h) - 12\lambda_{hhhh}A(m_h)\}. \quad \text{(A48)}$$

B. The hZZ form factors

The 1PI diagrams of the top-loop contribution to $M_1^{hZZ}(p_1^2, p_2^2, q^2)$ is calculated as

$$\begin{aligned}
M_1^{hZZ}(p_1^2, p_2^2, q^2) = &+\frac{1}{16\pi^2}\frac{32N_c m_f^2 m_Z^2}{v^3}\Bigg[\left\{\frac{1}{2}I_f^2 - I_f Q_f s_W^2 + Q_f^2 s_W^4\right\}\{2p_1^2 C_{21} + 2p_2^2 C_{22} + 4p_1 p_2 C_{23} + 2(D-2)C_{24} \\
&+ (3p_1^2 + p_1 p_2)C_{11} + (3p_1 p_2 + p_2^2)C_{12} + (p_1^2 + p_1 p_2)C_0\} + (I_f Q_f s_W^2 - Q_f^2 s_W^4)\{p_1^2 C_{21} + p_2^2 C_{22} \\
&+ 2p_1 p_2 C_{23} + DC_{24} + (p_1^2 + p_1 p_2)C_{11} + (p_1 p_2 + p_2^2)C_{12} + m_f^2 C_0\}\Bigg](p_1^2, p_2^2, q^2; m_f, m_f, m_f) \\
&+\frac{1}{16\pi^2}\frac{m_Z^2}{v^2}[2\cos^2 2\theta_W \lambda_{hw^+w^-} B_0(q; m_{w^\pm}, m_{w^\pm}) + 2\lambda_{hzz} B_0(q; m_z, m_z) + 6\lambda_{hhh} B_0(q; m_h, m_h) \\
&- 8\cos^2 2\theta_W \lambda_{hw^+w^-} C_{24}(p_1^2, p_2^2, q^2; m_{w^\pm}, m_{w^\pm}, m_{w^\pm}) - 8\lambda_{hzz} C_{24}(p_1^2, p_2^2, q^2; m_z, m_h, m_z) \\
&- 24\lambda_{hhh} C_{24}(p_1^2, p_2^2, q^2; m_h, m_z, m_h)],
\end{aligned} \tag{A49}$$

$$\begin{aligned}
M_2^{hZZ}(p_1^2, p_2^2, q^2) = &-\frac{1}{16\pi^2}\frac{32N_c m_f^2 m_Z^4}{v^3}\Bigg[\left\{\frac{1}{2}I_f^2 - I_f Q_f s_W^2 + Q_f^2 s_W^4\right\}\{4C_{23} + 3C_{12} + C_{11} + C_0\} \\
&+ (I_f Q_f s_W^2 - Q_f^2 s_W^4)\{C_{11} - C_{12}\}\Bigg](p_1^2, p_2^2, q^2; m_f, m_f, m_f) \\
&+\frac{1}{16\pi^2}\frac{m_Z^4}{v^2}[-8\cos^2 2\theta_W \lambda_{hw^+w^-} C_{1223}(p_1^2, p_2^2, q^2; m_{w^\pm}, m_{w^\pm}, m_{w^\pm}) \\
&- 8\lambda_{hzz} C_{1223}(p_1^2, p_2^2, q^2; m_z, m_h, m_z) - 24\lambda_{hhh} C_{1223}(p_1^2, p_2^2, q^2; m_h, m_z, m_h)],
\end{aligned} \tag{A50}$$

where $C_{1223} = C_{12} + C_{23}$, and

$$M_3^{hZZ}(p_1^2, p_2^2, q^2) = -\frac{1}{16\pi^2}\frac{32N_c m_f^2 m_Z^4}{v^3}\left(\frac{1}{2}I_f^2 - I_f Q_f s_W^2\right)\{C_{12} - C_{11} - C_0\}(p_1^2, p_2^2, q^2; m_f, m_f, m_f). \tag{A51}$$

C. The 1PI hhh form factor

The 1PI top-loop contribution to the hhh coupling is calculated as

$$\begin{aligned}
\Gamma_{hhh}^{1\mathrm{PI}}(p_1^2, p_2^2, q^2) = &-\sum_{f=t,b}\Bigg[\frac{1}{16\pi^2}\frac{8N_c m_f^4}{v^3}\{3(p_1^2 C_{21} + p_2^2 C_{22} + 2p_1 p_2 C_{23} + DC_{24}) + (4p_1^2 + 2p_1 p_2)C_{11} \\
&+ (2p_2^2 + 4p_1 p_2)C_{12} + (m_f^2 + p_1^2 + p_1 p_2)C_0\}\Bigg](p_1^2, p_2^2, q^2; m_f, m_f, m_f) \\
&+\frac{1}{16\pi^2}[+2\lambda_{hw^+w^-}\lambda_{hhw^+w^-}\{B_0(q^2; m_{w^\pm}, m_{w^\pm}) + B_0(p_1^2; m_{w^\pm}, m_{w^\pm}) + B_0(p_2^2; m_{w^\pm}, m_{w^\pm})\} \\
&- 2\lambda_{hw^+w^-}^3 C_0(p_1^2, p_2^2, q^2; m_{w^\pm}, m_{w^\pm}, m_{w^\pm}) + 4\lambda_{hzz}\lambda_{hhzz}\{B_0(q^2; m_z, m_z) + B_0(p_1^2; m_z, m_z) \\
&+ B_0(p_2^2; m_z, m_z)\} - 4\lambda_{hzz}^3 C_0(p_1^2, p_2^2, q^2; m_z, m_z, m_z) + 72\lambda_{hhh}\lambda_{hhhh}\{B_0(q^2; m_h, m_h) \\
&+ B_0(p_1^2; m_h, m_h) + B_0(p_2^2; m_h, m_h)\} - 108\lambda_{hhh}^3 C_0(p_1^2, p_2^2, q^2; m_h, m_h, m_h)].
\end{aligned} \tag{A52}$$

APPENDIX B: IN THE TWO HIGGS DOUBLET MODEL

The kinetic and mass terms of the bare Higgs Lagrangian is written in terms of the renormalized quantities and the counterterm parameters as

$$\mathcal{L}_{\rm Higgs} \to \mathcal{L}_{\rm Higgs} + \delta T_h h + \delta T_H H + \frac{1}{2}\left\{(p^2 - m_h^2)\delta Z_h - \delta m_h^2 + \frac{\sin^2\alpha}{\cos\beta}\frac{\delta T_1}{v} + \frac{\cos^2\alpha}{\sin\beta}\frac{\delta T_2}{v}\right\}h^2 + \frac{1}{2}\left\{(p^2 - m_H^2)\delta Z_H - \delta m_H^2 + \frac{\cos^2\alpha}{\cos\beta}\frac{\delta T_1}{v} + \frac{\sin^2\alpha}{\sin\beta}\frac{\delta T_2}{v}\right\}H^2 + \left\{(2p^2 - m_h^2 - m_H^2)\delta C_h - (m_H^2 - m_h^2)\delta\alpha + \cos\alpha\sin\alpha\left(-\frac{1}{\cos\beta}\frac{\delta T_1}{v} + \frac{1}{\sin\beta}\frac{\delta T_2}{v}\right)\right\}Hh + \frac{1}{2}\left\{p^2\delta Z_z + \cos\beta\frac{\delta T_1}{v} + \sin\beta\frac{\delta T_2}{v}\right\}z^2 + \frac{1}{2}\left\{(p^2 - m_A^2)\delta Z_A - \delta m_A^2 + \left(\frac{\sin^2\beta}{\cos\beta} - \cos\beta + \frac{1}{\cos\beta}\right)\frac{\delta T_1}{2v} + \left(\frac{\cos^2\beta}{\sin\beta} - \sin\beta + \frac{1}{\sin\beta}\right)\frac{\delta T_2}{2v}\right\}A^2 + \left\{(2p^2 - m_A^2)\delta C_A + m_A^2\delta\beta - \sin\beta\frac{\delta T_1}{v} + \cos\beta\frac{\delta T_2}{v}\right\}zA + \left\{p^2\delta Z_{w^\pm} + \cos\beta\frac{\delta T_1}{v} + \sin\beta\frac{\delta T_2}{v}\right\}w^+w^- + \left\{(p^2 - m_{H^\pm}^2)\delta Z_{H^\pm} - \delta m_{H^\pm}^2 + \left(\frac{\sin^2\beta}{\cos\beta} - \cos\beta + \frac{1}{\cos\beta}\right)\frac{\delta T_1}{2v} + \left(\frac{\cos^2\beta}{\sin\beta} - \sin\beta + \frac{1}{\sin\beta}\right)\frac{\delta T_2}{2v}\right\}H^+H^- + \left\{(2p^2 - m_{H^\pm}^2)\delta C_{H^+} + m_{H^\pm}^2\delta\beta - \sin\beta\frac{\delta T_1}{v} + \cos\beta\frac{\delta T_2}{v}\right\}(w^+H^- + H^+w^-), \tag{B1}$$

where

$$\delta T_1 = \cos\alpha\delta T_H - \sin\alpha\delta T_h, \tag{B2}$$

$$\delta T_2 = \sin\alpha\delta T_H + \cos\alpha\delta T_h. \tag{B3}$$

1. One- and two-point functions

The explicit expressions for the relevant 1PI diagrams are given in terms of the Passarino-Veltman functions[47] below. The Yukawa couplings are assumed to be of the Model II THDM [21].

$$\Pi_T^{ZZ}(p^2) = -\frac{N_c}{16\pi^2}\frac{16m_Z^2}{v^2}\left[\left(\frac{1}{2}I_f^2 - I_f Q_f s_W^2 + Q_f^2 s_W^4\right)\{(D-2)B_{22} + p^2(B_1 + B_{21})\} + (I_f - Q_f s_W^2)Q_f s_W^2 m_f^2 B_0\right] \times (p^2, m_f, m_f) + \frac{1}{16\pi^2}\frac{m_Z^2}{v^2}[\cos^2(\alpha-\beta)\{B_5(p^2; m_h, m_A) + B_5(p^2; m_H, m_z)\} + \sin^2(\alpha-\beta)\{B_5(p^2; m_h, m_z) + B_5(p^2; m_H, m_A)\} + c_{2W}^2\{B_5(p^2; m_{w^\pm}, m_{w^\pm}) + B_5(p^2; m_{H^\pm}, m_{H^\pm})\}], \tag{B4}$$

$$\Pi_T^{WW}(p^2) = -\frac{N_c}{16\pi^2}\frac{m_W^2}{v^2}\{(D-2)4B_{22} + 4p^2(B_1 + B_{21})\}(p^2; m_t, m_b) + \frac{1}{16\pi^2}\frac{m_W^2}{v^2}[\cos^2(\alpha-\beta)\{B_5(p^2; m_h, m_{H^\pm}) + B_5(p^2; m_H, m_{w^\pm})\} + \sin^2(\alpha-\beta)\{B_5(p^2; m_h, m_{w^\pm}) + B_5(p^2; m_H, m_{H^\pm})\} + B_5(p^2; m_z, m_{w^\pm}) + B_5(p^2; m_A, m_{H^\pm})]. \tag{B5}$$

$$T_h^{\rm 1PI} = -\frac{N_c}{16\pi^2}\frac{4m_t^2}{v}\frac{\cos\alpha}{\sin\beta}A(m_t) + \frac{N_c}{16\pi^2}\frac{4m_b^2}{v}\frac{\sin\alpha}{\cos\beta}A(m_b) - \frac{1}{16\pi^2}\{\lambda_{hH^+H^-}A(m_{H^\pm}) + \lambda_{hAA}A(m_A) + 3\lambda_{hhh}A(m_h) + \lambda_{hHH}A(m_H)\}, \tag{B6}$$

$$T_H^{\rm 1PI} = -\frac{N_c}{16\pi^2}\frac{4m_t^2}{v}\frac{\sin\alpha}{\sin\beta}A(m_t) - \frac{N_c}{16\pi^2}\frac{4m_b^2}{v}\frac{\cos\alpha}{\cos\beta}A(m_b) - \frac{1}{16\pi^2}\{\lambda_{HH^+H^-}A(m_{H^\pm}) + \lambda_{HAA}A(m_A) + \lambda_{Hhh}A(m_h) + 3\lambda_{HHH}A(m_H)\}. \tag{B7}$$

$$\Pi_{hh}^{\rm 1PI}(p^2) = -\frac{N_c}{16\pi^2}\Big[\frac{m_t^2}{v^2}\frac{\cos^2\alpha}{\sin^2\beta}\{4A(m_t) + (-2p^2 + 8m_t^2)B_0(p^2; m_t, m_t)\} + \frac{m_b^2}{v^2}\frac{\sin^2\alpha}{\cos^2\beta}\{4A(m_b) + (-2p^2 + 8m_b^2)B_0(p^2; m_b, m_b)\}\Big] + \frac{1}{16\pi^2}\{+(\lambda_{hH^+H^-})^2 B_0(p^2; m_{H^\pm}, m_{H^\pm}) + 2(\lambda_{hw^+H^-})^2 B_0(p^2; m_{w^\pm}, m_{H^\pm}) + (\lambda_{hw^+w^-})^2 B_0(p^2; m_{w^\pm}, m_{w^\pm}) - 2\lambda_{hhH^+H^-}A(m_{H^\pm}) + (\lambda_{hAA})^2 B_0(p^2; m_A, m_A) + 2(\lambda_{hzA})^2 B_0(p^2; m_z, m_A) + (\lambda_{hzz})^2 B_0(p^2; m_z, m_z) - 2\lambda_{hhAA}A(m_A) + (\lambda_{hHH})^2 B_0(p^2; m_H, m_H) + 4(\lambda_{hhH})^2 B_0(p^2; m_h, m_H) + 18(\lambda_{hhh})^2 B_0(p^2; m_h, m_h) - 12\lambda_{hhhh}A(m_h) - 2\lambda_{hhHH}A(m_H)\}. \tag{B8}$$

$$\Pi_{hH}^{\rm 1PI}(p^2) = -\frac{N_c}{16\pi^2}\Big[\frac{m_t^2}{v^2}\frac{\sin\alpha\cos\alpha}{\sin^2\beta}\{4A(m_t) + (-2p^2 + 8m_t^2)B_0(p^2; m_t, m_t)\} - \frac{m_b^2}{v^2}\frac{\sin\alpha\cos\alpha}{\cos^2\beta}\{4A(m_b) + (-2p^2 + 8m_b^2)B_0(p^2; m_b, m_b)\}\Big] + \frac{1}{16\pi^2}\{+\lambda_{hH^+H^-}\lambda_{HH^+H^-}B_0(p^2; m_{H^\pm}, m_{H^\pm}) + 2\lambda_{hw^+H^-}\lambda_{Hw^+H^-}B_0(p^2; m_{w^\pm}, m_{H^\pm}) + \lambda_{hw^+w^-}\lambda_{Hw^+w^-}B_0(p^2; m_{w^\pm}, m_{w^\pm}) - \lambda_{hHH^+H^-}A(m_{H^\pm}) + 2\lambda_{hAA}\lambda_{HAA}B_0(p^2; m_A, m_A) + \lambda_{hzA}\lambda_{HzA}B_0(p^2; m_z, m_A) + 2\lambda_{hzz}\lambda_{Hzz}B_0(p^2; m_A, m_A) - \lambda_{hHAA}A(m_A) + 6\lambda_{hHH}\lambda_{HHH}B_0(p^2; m_H, m_H) + 4\lambda_{hhH}\lambda_{hHH}B_0(p^2; m_h, m_H) + 6\lambda_{hhh}\lambda_{hhH}B_0(p^2; m_h, m_h) - 3\lambda_{hhhH}A(m_h) - 3\lambda_{hHHH}A(m_H)\}. \tag{B9}$$

$$\Pi_{zA}^{\rm 1PI}(p^2) = -\frac{N_c}{16\pi^2}\Big[\frac{m_t^2}{v^2}\cot\beta\{4A(m_t) - 2p^2B_0(p^2; m_t, m_t)\} - \frac{m_b^2}{v^2}\tan\beta\{4A(m_b) - 2p^2B_0(p^2; m_b, m_b)\}\Big] + \frac{1}{16\pi^2}\{-\lambda_{zAH^+H^-}A(m_{H^\pm}) + 2\lambda_{HzA}\lambda_{HAA}B_0(p^2; m_A, m_H) + 2\lambda_{hzA}\lambda_{hAA}B_0(p^2; m_A, m_h) - 3\lambda_{zAAA}A(m_A) + 2\lambda_{Hzz}\lambda_{HzA}B_0(p^2; m_z, m_H) + 2\lambda_{hzz}\lambda_{hzA}B_0(p^2; m_z, m_h) - \lambda_{HHzA}A(m_H) - \lambda_{hhzA}A(m_h)\}. \tag{B10}$$

A. The Z-A mixing

The expression of the form factor Γ_{ZA} of the Z-A mixing is given as

$$\Gamma_{ZA} = i\frac{1}{16\pi^2}\Big\{-\frac{m_Z}{v}\cos(\alpha-\beta)\lambda_{hAA}(2B_1 + B_0)(p^2; m_h, m_A) - \frac{m_Z}{v}\sin(\alpha-\beta)\lambda_{HAA}(2B_1 + B_0)(p^2; m_H, m_A) + \frac{m_Z}{v}\sin(\alpha-\beta)\lambda_{hzA}(2B_1 + B_0)(p^2; m_h, m_z) - \frac{m_Z}{v}\cos(\alpha-\beta)\lambda_{HzA}(2B_1 + B_0)(p^2; m_H, m_z) + \sum_q N_c\frac{4m_Z m_q}{v}c_{Aq\bar{q}}I_q B_0(p^2; m_q, m_q)\Big\}, \tag{B11}$$

where I_q is the isospin of the quark q, $c_{At\bar{t}} = -\frac{m_t}{v}\cot\beta$, and $c_{Ab\bar{b}} = -\frac{m_b}{v}\tan\beta$ in the Model II THDM, and the Higgs self-couplings λ_{hAA}, λ_{HAA}, λ_{hzA}, and λ_{HzA} are listed in Appendix E.

2. The *hZZ* vertex

The explicit expressions for the 1PI diagrams of the form factors of the hZZ vertex are given in terms of the Passarino-Veltman functions [47] by

$$
\begin{aligned}
M_1^{hZZ}(p_1^2, p_2^2, q^2) = &+\frac{1}{16\pi^2}\frac{32N_c m_f^2 m_Z^2}{v^3} c_{hf\bar{f}}\Bigg[\left\{\frac{1}{2}I_f^2 - I_f Q_f s_W^2 + Q_f^2 s_W^4\right\}\{2p_1^2 C_{21} + 2p_2^2 C_{22} + 4p_1 p_2 C_{23} + 2(D-2)C_{24} \\
&+ (3p_1^2 + p_1 p_2)C_{11} + (3p_1 p_2 + p_2^2)C_{12} + (p_1^2 + p_1 p_2)C_0\} + (I_f Q_f s_W^2 - Q_f^2 s_W^4)\{p_1^2 C_{21} + p_2^2 C_{22} \\
&+ 2p_1 p_2 C_{23} + DC_{24} + (p_1^2 + p_1 p_2)C_{11} + (p_1 p_2 + p_2^2)C_{12} + m_f^2 C_0\}\Bigg](p_1^2, p_2^2, q^2; m_f, m_f, m_f) \\
&+\frac{1}{16\pi^2}\frac{m_Z^2}{v^2}[2\cos^2 2\theta_W \lambda_{hH^+H^-} B_0(q; m_{H^\pm}, m_{H^\pm}) + 2\cos^2 2\theta_W \lambda_{hw^+w^-} B_0(q; m_{w^\pm}, m_{w^\pm}) \\
&+ 2\lambda_{hAA} B_0(q; m_A, m_A) + 2\lambda_{hzz} B_0(q; m_z, m_z) + 6\lambda_{hhh} B_0(q; m_h, m_h) + 2\lambda_{hHH} B_0(q; m_H, m_H) \\
&- 8\cos^2 2\theta_W \lambda_{hH^+H^-} C_{24}(p_1^2, p_2^2, q^2; m_{H^\pm}, m_{H^\pm}, m_{H^\pm}) \\
&- 8\cos^2 2\theta_W \lambda_{hw^+w^-} C_{24}(p_1^2, p_2^2, q^2; m_{w^\pm}, m_{w^\pm}, m_{w^\pm}) - 8\sin^2(\alpha-\beta)\{\lambda_{hzz} C_{24}(p_1^2, p_2^2, q^2; m_z, m_h, m_z) \\
&+ \lambda_{hAA} C_{24}(p_1^2, p_2^2, q^2; m_A, m_H, m_A) + \lambda_{hHH} C_{24}(p_1^2, p_2^2, q^2; m_H, m_A, m_H) \\
&+ 3\lambda_{hhh} C_{24}(p_1^2, p_2^2, q^2; m_h, m_z, m_h)\} - 8\cos^2(\alpha-\beta)\{\lambda_{hAA} C_{24}(p_1^2, p_2^2, q^2; m_A, m_h, m_A) \\
&+ \lambda_{hzz} C_{24}(p_1^2, p_2^2, q^2; m_z, m_H, m_z) + \lambda_{hHH} C_{24}(p_1^2, p_2^2, q^2; m_H, m_z, m_H) \\
&+ 3\lambda_{hhh} C_{24}(p_1^2, p_2^2, q^2; m_h, m_A, m_h)\} + 4\cos(\alpha-\beta)\sin(\alpha-\beta)\{\lambda_{hzA} C_{24}(p_1^2, p_2^2, q^2; m_z, m_h, m_A) \\
&+ \lambda_{hzA} C_{24}(p_1^2, p_2^2, q^2; m_A, m_h, m_z) - \lambda_{hzA} C_{24}(p_1^2, p_2^2, q^2; m_z, m_H, m_A) \\
&- \lambda_{hzA} C_{24}(p_1^2, p_2^2, q^2; m_A, m_H, m_z) + 2\lambda_{hhH} C_{24}(p_1^2, p_2^2, q^2; m_h, m_z, m_H) \\
&+ 2\lambda_{hhH} C_{24}(p_1^2, p_2^2, q^2; m_H, m_z, m_h) - 2\lambda_{hhH} C_{24}(p_1^2, p_2^2, q^2; m_h, m_A, m_H) \\
&- 2\lambda_{hhH} C_{24}(p_1^2, p_2^2, q^2; m_H, m_A, m_h)\}],
\end{aligned}
\tag{B12}
$$

$$
\begin{aligned}
M_2^{hZZ}(p_1^2, p_2^2, q^2) = &-\frac{1}{16\pi^2}\frac{32N_c m_f^2 m_Z^4}{v^3} c_{hf\bar{f}}\Bigg[\left\{\frac{1}{2}I_f^2 - I_f Q_f s_W^2 + Q_f^2 s_W^4\right\}\{4C_{23} + 3C_{12} + C_{11} + C_0\} \\
&+ (I_f Q_f s_W^2 - Q_f^2 s_W^4)\{C_{11} - C_{12}\}\Bigg](p_1^2, p_2^2, q^2; m_f, m_f, m_f) \\
&+\frac{1}{16\pi^2}\frac{m_Z^4}{v^2}[-8\cos^2 2\theta_W \lambda_{hH^+H^-} C_{1223}(p_1^2, p_2^2, q^2; m_{H^\pm}, m_{H^\pm}, m_{H^\pm}) \\
&- 8\cos^2 2\theta_W \lambda_{hw^+w^-} C_{1223}(p_1^2, p_2^2, q^2; m_{w^\pm}, m_{w^\pm}, m_{w^\pm}) \\
&- 8\sin^2(\alpha-\beta)\{\lambda_{hzz} C_{1223}(p_1^2, p_2^2, q^2; m_z, m_h, m_z) + \lambda_{hAA} C_{1223}(p_1^2, p_2^2, q^2; m_A, m_H, m_A) \\
&+ \lambda_{hHH} C_{1223}(p_1^2, p_2^2, q^2; m_H, m_A, m_H) + 3\lambda_{hhh} C_{1223}(p_1^2, p_2^2, q^2; m_h, m_z, m_h)\} \\
&- 8\cos^2(\alpha-\beta)\{\lambda_{hAA} C_{1223}(p_1^2, p_2^2, q^2; m_A, m_h, m_A) + \lambda_{hzz} C_{1223}(p_1^2, p_2^2, q^2; m_z, m_H, m_z) \\
&+ \lambda_{hHH} C_{1223}(p_1^2, p_2^2, q^2; m_H, m_z, m_H) + 3\lambda_{hhh} C_{1223}(p_1^2, p_2^2, q^2; m_h, m_A, m_h)\} \\
&+ 4\cos(\alpha-\beta)\sin(\alpha-\beta)\{\lambda_{hzA} C_{1223}(p_1^2, p_2^2, q^2; m_z, m_h, m_A) + \lambda_{hzA} C_{1223}(p_1^2, p_2^2, q^2; m_A, m_h, m_z) \\
&- \lambda_{hzA} C_{1223}(p_1^2, p_2^2, q^2; m_z, m_H, m_A) - \lambda_{hzA} C_{1223}(p_1^2, p_2^2, q^2; m_A, m_H, m_z) \\
&+ 2\lambda_{hhH} C_{1223}(p_1^2, p_2^2, q^2; m_h, m_z, m_H) + 2\lambda_{hhH} C_{1223}(p_1^2, p_2^2, q^2; m_H, m_z, m_h) \\
&- 2\lambda_{hhH} C_{1223}(p_1^2, p_2^2, q^2; m_h, m_A, m_H) - 2\lambda_{hhH} C_{1223}(p_1^2, p_2^2, q^2; m_H, m_A, m_h)\}],
\end{aligned}
\tag{B13}
$$

$$
M_3^{hZZ}(p_1^2, p_2^2, q^2) = -\frac{1}{16\pi^2}\frac{32N_c m_f^2 m_Z^4}{v^3} c_{hf\bar{f}}\left(\frac{1}{2}I_f^2 - I_f Q_f s_W^2\right)\{C_{12} - C_{11} - C_0\}(p_1^2, p_2^2, q^2; m_f, m_f, m_f), \tag{B14}
$$

where $c_{ht\bar{t}} = \cos\alpha/\sin\beta$ and $c_{hb\bar{b}} = -\sin\alpha/\cos\beta$ in the Model II THDM, and each coupling constant of Higgs bosons is listed in Appendix E.

3. The 1PI *hhh* form factor

The explicit expression for the 1PI diagrams of the *hhh* form factor is given in terms of the Passarino-Veltman functions [47] by

$$\Gamma^{1\mathrm{PI}}_{hhh}(p_1^2, p_2^2, q^2) = -\sum_{f=t,b}\Big[\frac{1}{16\pi^2}\frac{8N_c m_f^4}{v^3}c^3_{hf\bar{f}}\{3(p_1^2C_{21} + p_2^2C_{22} + 2p_1p_2C_{23} + DC_{24}) + (4p_1^2 + 2p_1p_2)C_{11}$$
$$+ (2p_2^2 + 4p_1p_2)C_{12} + (m_f^2 + p_1^2 + p_1p_2)C_0\}\Big](p_1^2, p_2^2, q^2; m_f, m_f, m_f)$$
$$+ \frac{1}{16\pi^2}[2\lambda_{hH^+H^-}\lambda_{hhH^+H^-}\{B_0(q^2; m_{H^\pm}, m_{H^\pm}) + B_0(p_1^2; m_{H^\pm}, m_{H^\pm}) + B_0(p_2^2; m_{H^\pm}, m_{H^\pm})\}$$
$$+ 4\lambda_{hw^+H^-}\lambda_{hhw^+H^-}\{B_0(q^2; m_{w^\pm}, m_{H^\pm}) + B_0(p_1^2; m_{w^\pm}, m_{H^\pm}) + B_0(p_2^2; m_{w^\pm}, m_{H^\pm})\}$$
$$+ 2\lambda_{hw^+w^-}\lambda_{hhw^+w^-}\{B_0(q^2; m_{w^\pm}, m_{w^\pm}) + B_0(p_1^2; m_{w^\pm}, m_{w^\pm}) + B_0(p_2^2; m_{w^\pm}, m_{w^\pm})\}$$
$$- 2\lambda^3_{hH^+H^-}C_0(p_1^2, p_2^2, q^2; m_{H^\pm}, m_{H^\pm}, m_{H^\pm}) - 2\lambda_{hH^+H^-}\lambda^2_{hw^+H^-}\{C_0(p_1^2, p_2^2, q^2; m_{H^\pm}, m_{H^\pm}, m_{w^\pm})$$
$$+ C_0(p_1^2, p_2^2, q^2; m_{H^\pm}, m_{w^\pm}, m_{H^\pm}) + C_0(p_1^2, p_2^2, q^2; m_{w^\pm}, m_{H^\pm}, m_{H^\pm})\}$$
$$- 2\lambda_{hw^+w^-}\lambda^2_{hw^+H^-}\{C_0(p_1^2, p_2^2, q^2; m_{H^\pm}, m_{w^\pm}, m_{w^\pm}) + C_0(p_1^2, p_2^2, q^2; m_{w^\pm}, m_{H^\pm}, m_{w^\pm})$$
$$+ C_0(p_1^2, p_2^2, q^2; m_{w^\pm}, m_{w^\pm}, m_{H^\pm})\} - 2\lambda^3_{hw^+w^-}C_0(p_1^2, p_2^2, q^2; m_{w^\pm}, m_{w^\pm}, m_{w^\pm})$$
$$+ 4\lambda_{hAA}\lambda_{hhAA}\{B_0(q^2; m_A, m_A) + B_0(p_1^2; m_A, m_A) + B_0(p_2^2; m_A, m_A)\} + 2\lambda_{hzA}\lambda_{hhzA}\{B_0(q^2; m_z, m_A)$$
$$+ B_0(p_1^2; m_z, m_A) + B_0(p_2^2; m_z, m_A)\} + 4\lambda_{hzz}\lambda_{hhzz}\{B_0(q^2; m_z, m_z) + B_0(p_1^2; m_z, m_z)$$
$$+ B_0(p_2^2; m_z, m_z)\} - 4\lambda^3_{hAA}C_0(p_1^2, p_2^2, q^2; m_A, m_A, m_A) - 2\lambda_{hAA}\lambda^2_{hzA}\{C_0(p_1^2, p_2^2, q^2; m_A, m_A, m_z)$$
$$+ C_0(p_1^2, p_2^2, q^2; m_A, m_z, m_A) + C_0(p_1^2, p_2^2, q^2; m_z, m_A, m_A)\} - 2\lambda_{hzz}\lambda^2_{hzA}\{C_0(p_1^2, p_2^2, q^2; m_A, m_z, m_z)$$
$$+ C_0(p_1^2, p_2^2, q^2; m_z, m_A, m_z) + C_0(p_1^2, p_2^2, q^2; m_z, m_z, m_A)\} - 4\lambda^3_{hzz}C_0(p_1^2, p_2^2, q^2; m_z, m_z, m_z)$$
$$+ 4\lambda_{hHH}\lambda_{hhHH}\{B_0(q^2; m_H, m_H) + B_0(p_1^2; m_H, m_H) + B_0(p_2^2; m_H, m_H)\}$$
$$+ 12\lambda_{hhH}\lambda_{hhhH}\{B_0(q^2; m_h, m_H) + B_0(p_1^2; m_h, m_H) + B_0(p_2^2; m_h, m_H)\} + 72\lambda_{hhh}\lambda_{hhhh}\{B_0(q^2; m_h, m_h)$$
$$+ B_0(p_1^2; m_h, m_h) + B_0(p_2^2; m_h, m_h)\} - 108\lambda^3_{hhh}C_0(p_1^2, p_2^2, q^2; m_h, m_h, m_h)$$
$$- 24\lambda_{hhh}\lambda^2_{hhH}\{C_0(p_1^2, p_2^2, q^2; m_H, m_h, m_h) + C_0(p_1^2, p_2^2, q^2; m_h, m_H, m_h) + C_0(p_1^2, p_2^2, q^2; m_h, m_h, m_H)\}$$
$$- 8\lambda_{hHH}\lambda^2_{hhH}\{C_0(p_1^2, p_2^2, q^2; m_H, m_h, m_H) + C_0(p_1^2, p_2^2, q^2; m_H, m_H, m_h) +$$
$$C_0(p_1^2, p_2^2, q^2; m_h, m_H, m_H)\} - 4\lambda^3_{hHH}C_0(p_1^2, p_2^2, q^2; m_H, m_H, m_H)], \tag{B15}$$

where $c_{ht\bar{t}} = \cos\alpha/\sin\beta$ and $c_{hb\bar{b}} = -\sin\alpha/\cos\beta$ in the Model II THDM, and each coupling constant of Higgs bosons is listed in Appendix E.

APPENDIX C: WAVE FUNCTION RENORMALIZATION

Let us consider the wave functions of h and H. The bare scalars satisfy

$$\begin{bmatrix} h_{1B} \\ h_{2B} \end{bmatrix} = \begin{bmatrix} \cos\alpha_B & -\sin\alpha_B \\ \sin\alpha_B & \cos\alpha_B \end{bmatrix}\begin{bmatrix} H_B \\ h_B \end{bmatrix} = R(\alpha_B)\begin{bmatrix} H_B \\ h_B \end{bmatrix}. \tag{C1}$$

We can write

$$\begin{bmatrix} H_B \\ h_B \end{bmatrix} = R(-\alpha_B)\begin{bmatrix} h_{1B} \\ h_{2B} \end{bmatrix} = R(-\delta\alpha)R(-\alpha)\begin{bmatrix} h_{1B} \\ h_{2B} \end{bmatrix}$$
$$\to R(-\delta\alpha)R(-\alpha)\tilde{Z}\begin{bmatrix} h_1 \\ h_2 \end{bmatrix} = R(-\delta\alpha)Z\begin{bmatrix} H \\ h \end{bmatrix}, \tag{C2}$$

where $\tilde{Z}$ is an arbitrary real symmetric matrix, so that

$$Z = R(-\alpha)\tilde{Z}R(\alpha) \equiv \begin{bmatrix} Z_{HH}^{1/2} & Z_{Hh}^{1/2} \\ Z_{hH}^{1/2} & Z_{hh}^{1/2} \end{bmatrix} \tag{C3}$$

is also arbitrary symmetric ($Z_{hH} = Z_{Hh}$). We may expand these elements by

$$Z_{HH} = 1 + \delta Z_H + \cdots, \tag{C4}$$

$$Z_{hh} = 1 + \delta Z_h + \cdots, \tag{C5}$$

$$Z_{Hh} = 0 + \delta C_h + \cdots. \tag{C6}$$

In this way, we obtain Eq. (40).

APPENDIX D: PERTURBATIVE UNITARITY

The condition of perturbative unitarity has originally been discussed for the elastic scattering of the longitudinally polarized gauge bosons and the Higgs boson by Lee, Quigg, and Thacker [34]. The channels $W_L^+W_L^-$, Z_LZ_L, Z_Lh, hh are considered as the initial and final states, and the condition in Eq. (98) with $\xi = 1$ is imposed to each eigenvalue of the 4×4 S matrix.

The extension to the THDM has been studied by several authors [35,36]. The 14 channels,

$$\begin{aligned} &W_L^+W_L^-, \quad W_L^+H^-, \quad H^+W_L^-, \quad H^+H^-, \\ &Z_LZ_L, \quad Z_LA, \quad AA, \quad Z_Lh, \quad Z_LH, \\ &Ah, \quad AH, \quad hh, \quad hH, \quad HH, \end{aligned} \tag{D1}$$

have been taken into account, and the equivalence theorem [48,49] has been employed to evaluate the tree level S-wave amplitudes for each channel in Ref. [35]. The 14 eigenvalues of the S matrix are calculated and their expressions are given in terms of the Higgs coupling constants by

$$a_\pm = \frac{1}{16\pi}\left\{\frac{3}{2}(\lambda_1+\lambda_2) \pm \sqrt{\frac{9}{4}(\lambda_1-\lambda_2)^2 + (2\lambda_3+\lambda_4)^2}\right\}, \tag{D2}$$

$$b_\pm = \frac{1}{16\pi}\left\{\frac{1}{2}(\lambda_1+\lambda_2) \pm \sqrt{\frac{1}{4}(\lambda_1-\lambda_2)^2 + \lambda_4^2}\right\}, \tag{D3}$$

$$c_\pm = d_\pm = \frac{1}{16\pi}\left\{\frac{1}{2}(\lambda_1+\lambda_2) \pm \sqrt{\frac{1}{4}(\lambda_1-\lambda_2)^2 + \lambda_5^2}\right\}, \tag{D4}$$

$$e_1 = \frac{1}{16\pi}(\lambda_3 + 2\lambda_4 - 3\lambda_5), \tag{D5}$$

$$e_2 = \frac{1}{16\pi}(\lambda_3 - \lambda_5), \tag{D6}$$

$$f_+ = \frac{1}{16\pi}(\lambda_3 + 2\lambda_4 + 3\lambda_5), \tag{D7}$$

$$f_- = \frac{1}{16\pi}(\lambda_3 + \lambda_5), \tag{D8}$$

$$f_1 = f_2 = \frac{1}{16\pi}(\lambda_3 + \lambda_4). \tag{D9}$$

The perturbative unitarity condition is then expressed by

$$\begin{aligned} &|a_\pm|, \quad |b_\pm|, \quad |c_\pm|, \quad |d_\pm|, \\ &|e_{1,2}|, \quad |f_\pm|, \quad |f_{1,2}| < \xi. \end{aligned} \tag{D10}$$

The condition in (D10) with the tree level mass formulas in Eqs. (23) to (27) constrains the parameter space of the Higgs sector. The parameter ξ is taken to be $1/2$ in our numerical evaluation [21].

APPENDIX E: HIGGS COUPLINGS IN THE THDM

Here, we list the Higgs boson self-coupling constants in the THDM, which are expressed in terms of our input parameters.

1. Trilinear Higgs couplings

$$\lambda_{hhh} = -\frac{1}{4v\sin 2\beta}[\{\cos(3\alpha-\beta) + 3\cos(\alpha+\beta)\}m_h^2 - 4\cos^2(\alpha-\beta)\cos(\alpha+\beta)M^2], \tag{E1}$$

$$\lambda_{hHH} = -\frac{\sin(\alpha-\beta)}{2v\sin 2\beta}[\sin 2\alpha(m_h^2+2m_H^2) - (3\sin 2\alpha + \sin 2\beta)M^2], \tag{E2}$$

$$\lambda_{Hhh} = -\frac{\cos(\alpha-\beta)}{2v\sin 2\beta}[\sin 2\alpha(2m_h^2+m_H^2) - (3\sin 2\alpha - \sin 2\beta)M^2], \tag{E3}$$

$$\lambda_{HHH} = \frac{1}{4v\sin 2\beta}[\{\sin(3\alpha-\beta) - 3\sin(\alpha+\beta)\}m_H^2 + 4\sin^2(\alpha-\beta)\sin(\alpha+\beta)M^2], \tag{E4}$$

$$\lambda_{hAA} = -\frac{1}{4v\sin 2\beta}[\{\cos(\alpha-3\beta) + 3\cos(\alpha+\beta)\}m_h^2 - 4\sin 2\beta\sin(\alpha-\beta)m_A^2 - 4\cos(\alpha+\beta)M^2], \tag{E5}$$

$$\lambda_{HAA} = -\frac{1}{4v\sin 2\beta}[\{\sin(\alpha-3\beta) + 3\sin(\alpha+\beta)\}m_H^2 + 4\sin 2\beta\cos(\alpha-\beta)m_A^2 - 4\sin(\alpha+\beta)M^2], \tag{E6}$$

$$\lambda_{hzz} = \frac{m_h^2}{2v}\sin(\alpha-\beta), \tag{E7}$$

$$\lambda_{Hzz} = -\frac{m_H^2}{2v}\cos(\alpha-\beta), \tag{E8}$$

$$\lambda_{hzA} = \frac{m_A^2 - m_h^2}{v}\cos(\alpha-\beta), \tag{E9}$$

$$\lambda_{HzA} = \frac{m_A^2 - m_H^2}{v}\sin(\alpha-\beta), \tag{E10}$$

$$\lambda_{hH^+H^-} = -\frac{1}{2v\sin 2\beta}[\{\cos(\alpha-3\beta) + 3\cos(\alpha+\beta)\}m_h^2 - 4\sin 2\beta\sin(\alpha-\beta)m_{H^\pm}^2 - 4\cos(\alpha+\beta)M^2], \tag{E11}$$

$$\lambda_{HH^+H^-} = -\frac{1}{2v\sin 2\beta}[\{\sin(\alpha-3\beta)+3\sin(\alpha+\beta)\}m_H^2 + 4\sin 2\beta\cos(\alpha-\beta)m_{H^\pm}^2 - 4\sin(\alpha+\beta)M^2], \tag{E12}$$

$$\lambda_{hw^+w^-} = \frac{m_h^2}{v}\sin(\alpha-\beta), \tag{E13}$$

$$\lambda_{Hw^+w^-} = -\frac{m_H^2}{v}\cos(\alpha-\beta), \tag{E14}$$

$$\lambda_{hw^+H^-} = \frac{m_{H^\pm}^2 - m_h^2}{v}\cos(\alpha-\beta), \tag{E15}$$

$$\lambda_{Hw^+H^-} = \frac{m_{H^\pm}^2 - m_H^2}{v}\sin(\alpha-\beta). \tag{E16}$$

2. Quartic couplings

$$\lambda_{hhhh} = -\frac{1}{32v^2\sin^2 2\beta}[\{\cos(3\alpha-\beta) + 3\cos(\alpha+\beta)\}^2 m_h^2 + 4\sin^2 2\alpha\cos^2(\alpha-\beta)m_H^2 - 4(\cos 2\alpha+\cos 2\beta)^2 M^2], \tag{E17}$$

$$\lambda_{hhhH} = -\frac{\sin 2\alpha\cos(\alpha-\beta)}{4v^2\sin^2 2\beta}[\{\cos(3\alpha-\beta) + 3\cos(\alpha+\beta)\}m_h^2 + 2\sin 2\alpha\sin(\alpha-\beta)m_H^2 - 4\cos(\alpha+\beta)M^2], \tag{E18}$$

$$\lambda_{hhHH} = -\frac{1}{16v^2\sin^2 2\beta}[\sin 2\alpha\{6\sin 2\alpha + 3\sin(4\alpha-2\beta) - \sin 2\beta\}m_h^2 + \sin 2\alpha\{6\sin 2\alpha - 3\sin(4\alpha-2\beta) + \sin 2\beta\}m_H^2 - 2(2-3\cos 4\alpha+\cos 4\beta)M^2], \tag{E19}$$

$$\lambda_{zAAA} = -\frac{1}{8v^2\sin 2\beta}[\{3\cos 2\alpha+\cos(2\alpha-4\beta) + 4\cos 2\beta\}m_h^2 - \{3\cos 2\alpha+\cos(2\alpha-4\beta) - 4\cos 2\beta\}m_H^2 - 8\cos 2\beta M^2], \tag{E20}$$

$$\lambda_{hhAA} = -\frac{1}{32v^2\sin^2 2\beta}[\{9+3\cos 4\alpha+6\cos(2\alpha-2\beta)+\cos(4\alpha-4\beta)+3\cos 4\beta+10\cos(2\alpha+2\beta)\}m_h^2 + 2\sin 2\beta\{3\sin 2\alpha+\sin(2\alpha-4\beta)+2\sin 2\beta\}m_H^2 + 16\sin^2 2\beta\sin^2(\alpha-\beta)m_A^2 + 2\{6+\cos(2\alpha-6\beta) + 2\cos(2\alpha-2\beta)+2\cos 4\beta+5\cos(2\alpha+2\beta)\}M^2], \tag{E21}$$

$$\lambda_{hhzz} = \frac{1}{16v^2\sin 2\beta}[\{2\sin 2\alpha+\sin(4\alpha-2\beta)-3\sin 2\beta\}m_h^2 - 4\sin 2\alpha\cos^2(\alpha-\beta)m_H^2 - 8\sin 2\beta\cos^2(\alpha-\beta)(m_A^2-M^2)], \tag{E22}$$

$$\lambda_{hhzA} = -\frac{\cos(\alpha-\beta)}{4v^2\sin 2\beta}[\{\cos(3\alpha-\beta)+3\cos(\alpha+\beta)\}m_h^2 + 2\sin 2\alpha\sin(\alpha-\beta)m_H^2 + 4\sin 2\beta\sin(\alpha-\beta)m_A^2 - 4\cos 2\beta\cos(\alpha-\beta)M^2], \tag{E23}$$

$$\lambda_{HHzA} = -\frac{\sin(\alpha-\beta)}{4v^2\sin 2\beta}[2\sin 2\alpha\cos(\alpha-\beta)m_h^2 - \{\sin(3\alpha-\beta)-3\sin(\alpha+\beta)\}m_H^2 - 4\sin 2\beta\cos(\alpha-\beta)m_A^2 - 4\cos 2\beta\sin(\alpha-\beta)M^2], \tag{E24}$$

$$\lambda_{hhH^+H^-} = -\frac{1}{16v^2\sin^2 2\beta}[\{9 + 3\cos 4\alpha + 6\cos(2\alpha - 2\beta) + \cos(4\alpha - 4\beta) + 3\cos 4\beta + 10\cos(2\alpha + 2\beta)\}m_h^2 + \{3 - 3\cos 4\alpha + 2\cos(2\alpha - 2\beta) - \cos(4\alpha - 4\beta) + \cos 4\beta - 2\cos(2\alpha + 2\beta)\}m_H^2 + 16\sin^2(\alpha - \beta)\sin^2 2\beta m_{H^\pm}^2 - 2\{6 + \cos(2\alpha - 6\beta) + 2\cos(2\alpha - 2\beta) + 2\cos 4\beta + 5\cos(2\alpha + 2\beta)\}M^2], \tag{E25}$$

$$\lambda_{hhw^+w^-} = \frac{1}{8v^2\sin 2\beta}[\{2\sin 2\alpha + \sin(4\alpha - 2\beta) - 3\sin 2\beta\}m_h^2 - 4\sin 2\alpha\cos^2(\alpha - \beta)m_H^2 - 8\sin 2\beta\cos^2(\alpha - \beta)(m_{H^\pm}^2 - M^2)], \tag{E26}$$

$$\lambda_{hhw^+H^-} = -\frac{\cos(\alpha - \beta)}{4v^2\sin 2\beta}[\{\cos(3\alpha - \beta) + 3\cos(\alpha + \beta)\}m_h^2 + 2\sin 2\alpha\sin(\alpha - \beta)m_H^2 + 4\sin 2\beta\sin(\alpha - \beta)m_{H^\pm}^2 - 4\cos 2\beta\cos(\alpha - \beta)M^2], \tag{E27}$$

$$\lambda_{hHH^+H^-} = -\frac{1}{4v^2\sin^2 2\beta}[\sin 2\alpha\{3\cos 2\alpha + \cos(2\alpha - 4\beta) + 4\cos 2\beta\}m_h^2 + \sin 2\alpha\{-3\cos 2\alpha - \cos(2\alpha - 4\beta) + 4\cos 2\beta\}m_H^2 - 4\sin^2 2\beta\sin(2\alpha - 2\beta)m_{H^\pm}^2 - 4\{2\sin 2\alpha\cos^3 2\beta + \sin^2 2\beta\sin(2\alpha + 2\beta)\}M^2], \tag{E28}$$

$$\lambda_{zAH^+H^-} = -\frac{1}{4v^2\sin 2\beta}[\{3\cos 2\alpha + \cos(2\alpha - 4\beta) + 4\cos 2\beta\}m_h^2 - \{3\cos 2\alpha + \cos(2\alpha - 4\beta) - 4\cos 2\beta\}m_H^2 - 8\cos 2\beta M^2]. \tag{E29}$$

[1] LEP Electroweak Working Group, http://lepewwg.web.cern.ch/LEPEWWG/.
[2] K. Abe *et al.*, hep-ph/0109166.
[3] J. A. Aguilar-Saavedra *et al.*, hep-ph/0106315.
[4] T. Abe *et al.*, hep-ex/0106055; hep-ex/0106056; hep-ex/0106057; hep-ex/0106058.
[5] J. Ellis, M. K. Gaillard, and D.V. Nanopoulos, Nucl. Phys. **B106**, 292 (1976); B. L. Ioffe and V. A. Khoze, Sov. J. Part. Nuclei **9**, 50 (1978); D. R. T. Jones and S. T. Petcov, Phys. Lett. **84B**, 440 (1979); R. N. Cahn and S. Dawson, Phys. Lett. **136B**, 196 (1984); G. L. Kane, W.W. Repko, and W. B. Rolnick, Phys. Lett. **148B**, 367 (1984); R. N. Cahn, Nucl. Phys. **B255**, 341 (1985); B. A. Kniehl, Z. Phys. C **55**, 605 (1992); W. Kilian, M. Krämer, and P. M. Zerwas, Phys. Lett. B **373**, 135 (1996).
[6] M. Battaglia, E. Boos, and W. M. Yao, hep-ph/0111276, eConf C010630, E3016 (2001).
[7] S. Yamashita, "*A Study of Higgs Self-Coupling Measurement at about 1 TeV*" at LCWS2004, Paris, France, April 2004 (unpublished).
[8] Y. Yasui *et al.*, hep-ph/0211047.
[9] U. Baur, T. Plehn, and D. Rainwater, Phys. Rev. Lett. **89**, 151801 (2002); Phys. Rev. D **68**, 033001 (2003).
[10] F. Boudjema and A. Semenov, Phys. Rev. D **66**, 095007 (2002); M. N. Dubinin and A. Semenov, Eur. Phys. J. C **28**, 223 (2003).
[11] J. F. Gunion and H. E. Haber, Phys. Rev. D **67**, 075019 (2003).
[12] W. Hollik and S. Peñaranda, Eur. Phys. J. C **23**, 163 (2002); A. Dobado, M. J. Herrero, W. Hollik, and S. Peñaranda, Phys. Rev. D **66**, 095016 (2002).
[13] S. Kanemura, S. Kiyoura, Y. Okada, E. Senaha, and C.-P. Yuan, hep-ph/0209326.
[14] S. Kanemura, S. Kiyoura, Y. Okada, E. Senaha, and C.-P. Yuan, Phys. Lett. B **558**, 157 (2003).
[15] V. Barger, T. Han, P. Langacker, B. McElrath, and P. Zerwas, Phys. Rev. D **67**, 115001 (2003).
[16] A. Djouadi, H. E. Haber, and P. M. Zerwas, Phys. Lett. B **375**, 203 (1996); J. Kamoshita, Y. Okada, M. Tanaka, and I. Watanabe, hep-ph/9602224.
[17] A. Djouadi, W. Kilian, M. Muhlleitner, and P. M. Zerwas, Eur. Phys. J. C **10**, 27 (1999).
[18] G. Belánger *et al.*, Phys. Lett. B **576**, 152 (2003).
[19] G. Belánger *et al.*, Phys. Lett. B **571**, 163 (2003).
[20] G. Jikia, Nucl. Phys. **B412**, 57 (1994); R. Belusevic and G. Jikia, hep-ph/0403303 [Phys. Rev. D (to be published)].
[21] J. F. Gunion, H. E. Haber, G. Kane, and S. Dawson, *The Higgs Hunter's Guide* (Addison-Wesley, New York, 1990).
[22] H-J. He, C. T. Hill, and T. M. P. Tait, Phys. Rev. D **65**, 055006 (2002).
[23] A. G. Cohen, D. B. Kaplan, and A. E. Nelson, Annu. Rev. Nucl. Part. Sci. **43**, 27 (1993); A. T. Davies, C. D. Froggatt, G. Jenkins, and R. G. Moorhouse, Phys. Lett. B **336**, 464 (1994); K. Funakubo, A. Kakuto, and K.

Takenaga, Prog. Theor. Phys. **91**, 341 (1994); J. M. Cline, K. Kainulainen, and A. P. Vischer, Phys. Rev. D **54**, 2451 (1996).

[24] M. Hashimoto and S. Kanemura, Phys. Rev. D **70**, 055006 (2004).

[25] A. Zee, Phys. Lett. **161B**, 141 (1985); S. Kanemura, T. Kasai, G.-L. Lin, Y. Okada, J.-J. Tseng, and C.-P. Yuan, Phys. Rev. D **64**, 053007 (2001); K. Cheung and O. Seto, Phys. Rev. D **69**, 113009 (2004).

[26] S. Kiyoura and Y. Okada, hep-ph/0101172.

[27] K. I. Aoki, Z. Hioki, M. Konuma, R. Kawabe, and T. Muta, Prog. Theor. Phys. Suppl. **73**, 1 (1982); M. Böhm, H. Spiesberger, and W. Hollik, Fortschr. Phys. **34**, 687 (1986); W. Hollik, *ibid.* **38**, 165 (1990).

[28] P. H. Chankowski, S. Pokorski, and J. Rosiek, Nucl. Phys. **B423**, 437 (1994); R. Santos and A. Barrosa, Phys. Rev. D,**56** 5366 (1997).

[29] P. Ciafaloni and D. Espriu, Phys. Rev. D **56**, 1752 (1997).

[30] I. F. Ginzburg, M. Krawczyk, and P. Osland, hep-ph/0101331; hep-ph/9909455.

[31] A. Arhrib, M. Capdequi Peyranere, W. Hollik, and S. Penaranda, hep-ph/0307391.

[32] S. Kanemura and H.-A. Tohyama, Phys. Rev. D **57**, 2949 (1998); M. Malinsky, Acta Physica Slovaca **52**, 259 (2002); M. Malinsky and J. Horejsi, Eur. Phys. J. C **34**, 477 (2004).

[33] A. Arhrib, M. Capdequi Peyranere, W. Hollik, and G. Moultaka, Nucl. Phys. **B581**, 34 (2000); **B581**, 400(E) (2004); S. Kanemura, Phys. Rev. D **61**, 095001 (2000); Eur. Phys. J. C **17**, 473 (2000).

[34] B.W. Lee, C. Quigg, and H. B. Thacker, Phys. Rev. Lett. **38**, 883 (1977).

[35] S. Kanemura, T. Kubota, and E. Takasugi, Phys. Lett. B **313**, 155 (1993).

[36] H. Hüffel and G. Pocsik, Z. Phys. C **8**, 13 (1981); J. Maalampi, J. Sirkka, and I. Vilja, Phys. Lett. B **265**, 371 (1991); A. G. Akeroyd, A. Arhrib, and E.-M. Naimi, Phys. Lett. B **490**, 119 (2000); I. F. Ginzburg and I. P. Ivanov, hep-ph/0312374.

[37] N. G. Deshpande and E. Ma, Phys. Rev. D **18**, 2574 (1978); S. Nie and M. Sher, Phys. Lett. B **449**, 89 (1999).

[38] C. S. Lim, T. Inami, and N. Sakai, Phys. Rev. D **29**, 1488 (1984).

[39] P. H. Chankowski, M. Krawczyk, and J. Zochowski, Eur. Phys. J. C **11**, 661 (1999).

[40] T. Appelquist and J. Carazzone, Phys. Rev. D **11**, 2856 (1975).

[41] M. E. Peskin and T. Takeuchi, Phys. Rev. Lett. **65**, 964 (1990); Phys. Rev. D **46**, 381 (1992).

[42] I. F. Ginzburg, M. Krawczyk, and P. Osland, Nucl. Instrum. Methods Phys. Res., Sect. A **472**, 149 (2001).

[43] H. E. Haber and A. Pomarol, Phys. Lett. B **302**, 435 (1993); A. Pomarol and R. Vega, Nucl. Phys. **B413**, 3 (1994).

[44] M. Ciuchini, G. Degrassi, P. Gambini, and G. F. Giudice, Nucl. Phys. **B527**, 21 (1998); P. Ciafaloni, A. Romanino, and A. Strumia, Nucl. Phys. **B524**, 361 (1998); F. M. Borzumati and C. Greub, Phys. Rev. D **58**, 074004 (1998); T. M. Aliev and E. O. Iltan, Phys. Rev. D **58**, 095014 (1998).

[45] Y. Okada, "*New Physics from Higgs Self-Coupling Measurement*" at LCWS 2004, Paris, April 2004 (unpublished); S. Kanemura, Y. Okada, and E. Senaha, (to be published).

[46] S. Kanemura, T. Kasai, and Y. Okada, Phys. Lett. B **471**, 182 (1999); hep-ph/9911312.

[47] G. Passarino and M. Veltman, Nucl. Phys. **B160**, 151 (1979).

[48] J. M. Cornwall, D. N. Levin, and G. Tiktopoulos, Phys. Rev. Lett. **30**, 1268 (1973); Phys. Rev. D **10**, 1145 (1974); B.W. Lee, C. Quigg, and H. B. Thacker, Phys. Rev. D **16**, 1519 (1977).

[49] M. S. Chanowitz and M. K. Gaillard, Nucl. Phys. **B261**, 379 (1985); Y.P. Yao and C.-P. Yuan, Phys. Rev. D **38**, 2237 (1988); H. Veltman, Phys. Rev. D **41**, 2294 (1990); J. Bagger and C. Schmidt, Phys. Rev. D **41**, 264 (1990); H.-J. He, Y.-P. Kuang, and X. Li, Phys. Rev. Lett. **69**, 2619 (1992); Phys. Rev. D **49**, 4842 (1994).